ORIGINAL ARTICLE

Basic Study

Bone marrow mesenchymal stem cells induce M2 microglia polarization through PDGF-AA/MANF signaling

Fan Yang, Wen-Bin Li, Ye-Wei Qu, Jin-Xing Gao, Yu-Shi Tang, Dong-Jie Wang, Yu-Jun Pan

Fan Yang, Wen-Bin Li, Ye-Wei Qu, Jin-Xing Gao, Yu-Shi Tang, Yu-Jun Pan, Department of Neurology, The First Clinical College of Harbin Medical University, Harbin 150001, Heilongjiang Province, China

Dong-Jie Wang, Department of Respiratory Medicine, The First Clinical College of Harbin Medical University, Harbin 150001, Heilongjiang Province, China

Corresponding author: Yu-Jun Pan, PhD, Professor, Chief Doctor, Department of Neurology, The First Clinical College of Harbin Medical University, No. 23, Youzheng Street, Nangang District, Harbin 150001, Heilongjiang Province, China. yujunpan@ems.hrbmu.edu.cn

Abstract

BACKGROUND

Bone marrow mesenchymal stem cells (BMSCs) are capable of shifting the microglia/macrophages phenotype from M1 to M2, contributing to BMSCs-induced brain repair. However, the regulatory mechanism of BMSCs on microglia/macrophages after ischemic stroke is unclear. Recent evidence suggests that mesencephalic astrocyte–derived neurotrophic factor (MANF) and platelet-derived growth factor-AA (PDGF-AA)/MANF signaling regulate M1/M2 macrophage polarization.

AIM

To investigate whether and how MANF or PDGF-AA/MANF signaling influences BMSCs-mediated M2 polarization.

METHODS

We identified the secretion of MANF by BMSCs and developed transgenic BMSCs using a targeting small interfering RNA for knockdown of MANF expression. Using a rat middle cerebral artery occlusion (MCAO) model transplanted by BMSCs and BMSCs–microglia Transwell coculture system, the effect of BMSCs-induced downregulation of MANF expression on the phenotype of microglia/macrophages was tested by Western blot, quantitative reverse transcription-polymerase chain reaction, and immunofluorescence. Additionally, microglia were transfected with mimics of miR-30a*, which influenced expression of X-box binding protein (XBP) 1, a key transcription factor that synergized with activating transcription factor 6 (ATF6) to govern MANF expression. We examined the levels of miR-30a*, ATF6, XBP1, and MANF after PDGF-AA

treatment in the activated microglia.

RESULTS
Inhibition of MANF attenuated BMSCs-induced functional recovery and decreased M2 marker production, but increased M1 marker expression *in vivo* or *in vitro*. Furthermore, PDGF-AA treatment decreased miR-30a* expression, had no influence on the levels of ATF6, but enhanced expression of both XBP1 and MANF.

CONCLUSION
BMSCs-mediated MANF paracrine signaling, in particular the PDGF-AA/miR-30a*/XBP1/MANF pathway, synergistically mediates BMSCs-induced M2 polarization.

Key words: Mesencephalic astrocyte–derived neurotrophic factor; Bone marrow mesenchymal stem cell; Microglia/macrophage polarization; Endoplasmic reticulum stress; Cerebral ischemia/reperfusion injury

Core tip: Induction of M2 microglia/macrophage polarization may contribute to the mechanisms underlying the neuroprotective effect of bone marrow mesenchymal stem cells (BMSCs) in treating stroke. This is one of the few known studies exploring the soluble mediators responsible for interactions between BMSCs and microglia/macrophages. We demonstrated that BMSCs-mediated MANF paracrine signaling, in particular the PDGF-AA/miR-30a*/XBP1/MANF pathway, was involved in BMSCs-induced M2 phenotype polarization. Therefore, this novel molecular mechanism of BMSCs-based immunomodulatory effect on microglia/macrophages may be a novel promising therapeutic strategy for treatment of ischemic stroke.

INTRODUCTION

Ischemic stroke following cerebral artery occlusion is a major cause of chronic disability worldwide and effective therapy to improve functional recovery after stroke is not available[1]. Bone marrow mesenchymal stem cells (BMSCs) are well known as rare multipotent cells and are characterized as potent modulators of regeneration and immune responses. BMSCs transplantation may be an effective multitarget therapeutic strategy to facilitate functional recovery after ischemic stroke through pleiotropic mechanisms[2-4].

Classic (M1) or alternative (M2) activation has been mostly reported for macrophage responses during peripheral inflammation, and recently, microglia were found to have a similar activation process upon ischemic insult[5]. M1-like microglia/macrophages secrete proinflammatory cytokines, such as inducible nitric oxide synthase (iNOS), and cause tissue damage. In contrast, M2-like microglia/macrophages secrete anti-inflammatory cytokines, such as Arginase-1 (Arg-1), supporting neural repair[6,7]. Recently, several *in vitro*[8,9] and *in vivo*[10,11] studies have shown that BMSCs promote M2 polarization and neurogenesis and tissue repair, probably depending on the trophic and growth factors secreted by BMSCs. However, the precise mechanism underlying BMSCs-induced M2 polarization is not yet clear[12].

Mesencephalic astrocyte-derived neurotrophic factor (MANF), also named as arginine-rich, mutated in early stage tumor (ARMET), is a soluble protein induced by endoplasmic reticulum (ER) stress to protect against ER-stress-induced damage[13-17]. Treatment with MANF significantly reduces ischemic brain injury and improves behavior in stroke in rats[18-21]. ER stress triggers activation of unfolded protein

response (UPR), which comprises two prosurvival pathways that are controlled by stress sensor proteins in the ER membrane: Activating transcription factor 6 (ATF6) and inositol-requiring enzyme-1(IRE1)[22-24]. After activation, IRE1 converts to an active endonuclease that cleaves unspliced X-box binding protein-1 (XBP1u) mRNA into spliced XBP1 (XBP1s) mRNA, which encodes the transcriptionally active XBP1s protein[25]. ER stress-induced transcriptional upregulation of MANF is driven by an ER stress response element (ERSE)-II in the MANF promoter, and is recognized by ATF6 or XBP1s[26,27]. The XBP1 arm of the UPR is thought to play a critical role in enhancing the M2-like macrophage phenotype[28]. A recent study has shown that damaged retina secretes platelet-derived growth factor-AA (PDGF-AA) that signals to innate immune cells to produce MANF, which promotes macrophage M2 activation and tissue repair[29]. Based on these observations, it would be logical to propose that PDGF-AA, secreted abundantly from BMSCs[30], regulates XBP1 expression, which enhances expression of MANF, contributing to M2 phenotype.

MicroRNAs (miRNAs) are a new class of endogenous, small, 19-25-nucleotide noncoding RNAs that act as negative regulators of gene expression by inhibiting mRNA translation or promoting mRNA degradation[31]. As the first discovery of a miRNA that directly modulates a UPR effector, ER stress-inducible miR-30c-2* limits expression of XBP1, which is a potential target of the miR-30* family[32,33]. Therefore, we hypothesized that miR-30a* (recently designated as miR-30a-3p) might participate in the exquisite regulation of XBP1, and PDGF-AA might influence XBP1 *via* miR-30a*. Here, we aimed to explore whether BMSCs-mediated MANF paracrine signaling and the PDGF-AA/miR-30a*/XBP1/MANF axis can drive M2 polarization.

MATERIALS AND METHODS

Animals
Adult male Wistar rats, aged 6-7 wk and weighing 260-280 g, immature male Wistar rats, aged 4 wk and weighing 100-150 g, and neonatal Wistar rats were obtained from the Experimental Animal Center of the Second Clinical College of Harbin Medical University (Harbin, China) and housed in pathogen-free conditions. The rats were kept under standard conditions of temperature (25 ± 2°C) and lighting (12 h light/dark cycle). The Ethics Committee of the First Clinical College of Harbin Medical University approved this study (No. 2019006).

BMSCs isolation, culture, and identification
Rat BMSCs were isolated and cultured as described previously[4]. Bone marrow was obtained from the femurs and tibias taken from immature Wistar rats, followed by 5 min of centrifugation at 1500 rpm. The cell pellets were resuspended and cultured in Dulbecco's modified Eagle's medium (DMEM)/F12 (Invitrogen, Carlsbad, CA, United States) supplemented with 10% fetal bovine serum (FBS; Invitrogen) and 1% penicillin/streptomycin liquid (Invitrogen). Cells were seeded at 10^6/mL in a 25-cm^2 tissue culture flask. After 3 d of culture with 5% CO_2 at 37°C, nonadherent hematopoietic cells were removed, and the medium was replaced. Half of the medium was replaced every 3-4 d, and adherent cells were allowed to reach 80% confluence before they were subcultured after 0.25% trypsin–EDTA digestion (Sigma–Aldrich, St. Louis, MO, United States). The third- and fourth-generation cells were used for further experiments. To verify the phenotype of the isolated BMSCs, the cells were incubated with fluorescence-conjugated antibodies, including CD90–fluorescein isothiocyanate (FITC), CD73–FITC, CD45–FITC, and CD11b–phycoerythrin (PE) (1:100; Sigma–Aldrich). An isotype-matched antibody was used as a control. Labeled cells were analyzed using flow cytometry (Thermo Fisher Scientific, Waltham, MA, United States).

Genetic engineering of BMSCs
Small interfering RNAs (siRNAs) targeting rat MANF (siMANF1, siMANF2, siMANF3, and negative control; NC) were designed and synthesized by Genechem Co. Ltd. (Shanghai, China). SiRNA sequences for transient knockdown of MANF are: 5'-CAGGCGACTGCGAAGTTTGTA-3' for siMANF1 sense, 5'-AATCGGTTGTGCTACTACA TT-3' for siMANF2 sense, and 5'-CACCATATCCCT GTGGAGAAG-3' for siMANF3 sense. BMSCs were seeded at 70%-80% confluence 12 h before transfection. BMSCs were divided into five groups: Nontransfected BMSCs (control), siMANF1-transfected BMSCs, siMANF2-transfected BMSCs, siMANF3-transfected BMSCs, and NC-transfected BMSCs (BMSCs-NC). Cells were transfected

after seeding using Lipofectamine 2000 (Invitrogen). The final siRNA concentration was 50 nmol/L. After 48 h of transfection and antibiotics selection, cells were collected for protein and RNA extraction.

BMSCs transplantation

A total of 170 male adult Wistar rats were used. Mortality rate was about 22% during and after surgery, and 38 rats were excluded from the middle cerebral artery occlusion (MCAO) model. Specifically, seven rats died from bleeding from the jugular vein, 23 after surgery, and eight after anesthesia. Overall, 132 rats were randomly divided into six groups (n = 22): Sham operation, cerebral ischemia/reperfusion (I/R) injury, cerebral I/R injury with phosphate-buffered saline (PBS) treatment, cerebral I/R injury with BMSCs treatment, cerebral I/R injury with BMSCs-NC treatment, and cerebral I/R injury with BMSCs/siMANF treatment. The selected BMSCs, as well as those with the best efficiency of siRNA transfection, were prepared in PBS at 10^5 cells/µL and injected into the right striatum with a coordinate of 3 mm lateral to the midline, 0.4 mm anterior to the bregma, and 5 mm deep at a rate of 1 µL/min. For a shorter time to take effect, 10 µL of the cultured cells and the same volume of PBS were injected at 24 h before cerebral I/R injury. The needle was retained in place for 5 min after injection. The brain samples were collected from each group after 24 h of reperfusion for further analysis. An overview of *in vivo* experimental protocol is presented in Figure 1A.

MCAO

Focal cerebral I/R injury was induced by MCAO as described previously[4]. Animals were anesthetized with 3% pentobarbital sodium by intraperitoneal injection (40 mg/kg). The nylon threads (L3400) were purchased from Jialing Biotechnology Co. Ltd. (Guangzhou, China). The right common carotid artery, external carotid artery, and internal carotid artery were clearly isolated through a cervical midline incision. The thread was introduced into the end of the external carotid artery, and then the distal end of the external carotid artery was cut. After that, the thread was inserted to the internal carotid artery until showing a slight resistance. This was to ensure that the thread has already blocked the origin of the middle cerebral artery. After 2 h of ischemia, the suture was withdrawn to allow reperfusion. Sham-operated animals were subjected to the same procedure, except that the artery was not occluded. After surgery, the rats were kept in a warm box heated with lamps until they woke up and then returned to their home cages. Cerebral I/R injury model was evaluated after revival from anesthesia using the Zea-Longa suture-occluded method[34]. Rats with a neurological deficit score of 2-3 were considered to have had successful surgery and were used for further experiments.

Neurological function test

Behavioral recovery was assessed by a blinded observer using the modified Neurological Severity Scores (mNSS) and Bederson's score on days 1, 3, and 7 after MCAO surgery. mNSS was graded as 0-18 scores (0, normal; 18, maximal deficit). One score point represented an inability to perform a test or lack of a tested reflex[35]. Bederson's score was scored according to the following criteria[36]: 0, rats extend both forelimbs straight with no observable deficits; 1, rats keep the one forelimb to the breast and extend the other forelimb straight; 2, rats show decreased resistance to lateral push in addition to behavior in score 1 without circling; 3, rats twist the upper half of their body in addition to behavior in score 2.

Evaluation of infarct volume

After 7 d of reperfusion, the rats were killed, and the brains were rapidly removed and frozen at -80°C for 15 min. The frozen brains were cut into coronal 2-mm-thick sections. The brain slices were incubated in a 2% solution of 2,3,5-triphenylterazolium chloride (Sigma–Aldrich) in normal saline for 30 min at 37°C and then transferred to a 4% paraformaldehyde solution for fixation. After staining, digital photographs were taken. Areas of the infarction in each slice were measured with Image J software (National Institute of Health, Bethesda, MD, United States). In order to minimize the error caused by brain edema, the relative infarct volume percentage was calculated as (volume of contralateral-normal volume of ipsilateral)/volume of contralateral × 100%[37].

Microglia isolation and culture

The preparation of mixed glial cell cultures and the isolation of microglia were carried out according to Saura *et al*[38]. The brains of neonatal (P1–P3) rats were isolated, then
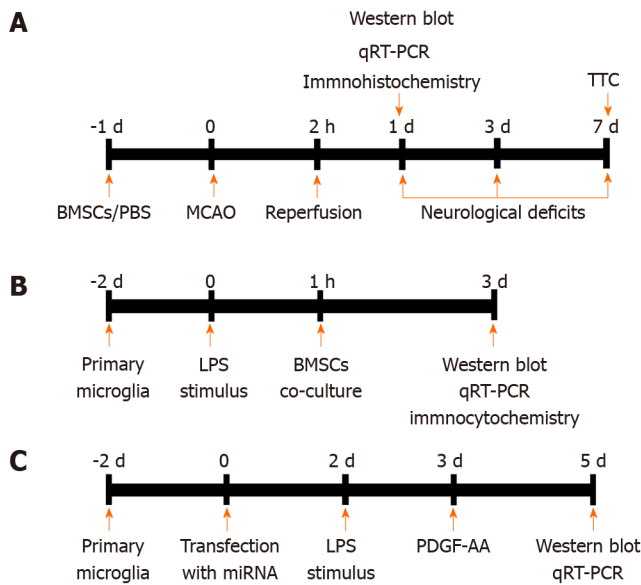
Figure 1 Experimental design. A: *In vivo* experiments. Bone marrow mesenchymal stem cells (BMSCs) or PBS were infused into the right striatum 1 d before MCAO. Animals were killed at 1 d for analysis by Western blot, qRT-PCR, and immunohistochemistry. Neurological function tests were evaluated at 1, 3, and 7 d post-stroke. Rats were killed at 7 d for TTC staining and measurement of infarct volume. B and C: *In vitro* experiments. Primary microglial cells were cultured for 2 d and exposed to 100 ng/mL LPS followed by indirect (Transwell) BMSCs coculture. After 2 d, cocultures were analyzed by Western blot, qRT-PCR, and immunocytochemistry (B). Cultured HAPI cells were transfected with miR-mimics, anti-miR, or corresponding negative control oligonucleotides for 24 h. PDGF-AA was added to the culture medium of HAPI cells pretreated with 100 ng/mL LPS for 24 h. After 2 d, cells were collected for Western blot and qRT-PCR (C). BMSCs: Bone marrow mesenchymal stem cells; PBS: Phosphate-buffered saline; MCAO: Middle cerebral artery occlusion; qRT-PCR: Real-time quantitative reverse transcription-polymerase chain reaction; TTC: 2,3,5-triphenylterazolium chloride; LPS: Lipopolysaccharide; PDGF-AA: Platelet-derived growth factor-AA.

the meninges and choroid plexus were removed. The rat cortices were digested by 0.05% trypsin–EDTA for 15 min at 37°C. After centrifuging at 1200 rpm for 2 min, the cells were plated in 75-cm^2 flasks that had been coated with poly-L-lysine (Invitrogen). After 48 h, the nonadherent cells were removed by thorough washing of the surface with culture medium. Mixed glial cells were cultured in DMEM supplemented with 10% FBS, 2 mmol/L L-glutamine (Sigma–Aldrich), and 1% penicillin/streptomycin at 37°C in 5% CO_2 in air and 95% humidity for 2 wk. The culture medium was changed every 3 d. To harvest pure microglia, microglia on the confluent mixed glial cell layer were isolated by shaking the flasks for 2 h at 180 rpm. The medium containing the layer of detached microglia was collected and immediately centrifuged for 2 min at 1200 rpm. The supernatant was removed, and the obtained pure microglia were resuspended in fresh culture medium and seeded into subcultures. Microglial harvesting was repeated for a maximum of three times at intervals of 3 d. The purity of our primary microglia culture was assessed by immunocytochemical staining for ionized calcium-binding adapter molecule (Iba1).

Microglia polarization and coculture assay

Microglia were harvested from flasks and seeded at 10^6 cells/well on a 24-well plate with DMEM containing 10% FBS. After 24 h, the medium was replaced with 1 mL of FBS-free medium, and the cells continued to grow for 24 h. Microglia were unstimulated or stimulated with lipopolysaccharide (LPS) (Sigma–Aldrich) at 100 ng/mL for 24 h before coculture with BMSCs. To investigate the effect of spatial separation, we prepared Transwell experiments, where 10^5 BMSCs were plated into Transwell chambers with 1-µm-pore-sized membranes suitable for 24-well plates (Millipore, Temecula, CA, United States) and 10^6 microglial cells were added to the lower compartment. Untreated microglia served as a control, and conditioned medium of BMSCs in the upper chamber served as a vehicle. After coculture for 48 h, microglia were collected for further analysis. The study design is briefly illustrated in Figure 1B.

HAPI cell culture and transfection

Rat microglia cell line (HAPI) from the American-Type Culture Collection (ATCC) (Manassas, VA, United States) was cultured in DMEM containing 10% FBS and 1% penicillin/streptomycin at 37°C in 5% CO_2. The miR-30a* oligonucleotides (mimics,

anti-miRNA, and corresponding NC) were prepared by Genechem. After 24 h of seeding HAPI cells in subculture (10^5 cells/well on a 24-well plate), transfection was performed using 100 nmol/L Lipofectamine 2000 (Invitrogen). HAPI cells were divided into five groups: Nontransfected microglia (control), miR-30a*-NC-transfected microglia (miR-NC), miR-30a*-mimics-transfected microglia (miR-mimics), anti-miR-NC-transfected microglia (anti-NC), and miR-30a*-inhibitor-transfected microglia (anti-miR). After 24 h of transfection, gene and protein expression was determined.

Treatment of transfected HAPI cells

To determine whether the level of MANF is affected by various concentrations of PDGF-AA, the activated HAPI cells were exposed to recombinant rat PDGF-AA (R&D Systems, Minneapolis, MN, United States) at 0.1, 1, and 10 ng/mL for 48 h. Expression of MANF was detected by Western blot. To investigate the effect of PDGF-AA on LPS-stimulated microglia, the transfected HAPI cells were stimulated for 24 h using LPS (100 ng/mL). PDGF-AA at the selected concentration was added to the cell culture medium of HAPI cells for 48 h. The study design is briefly illustrated in Figure 1C.

Immunofluorescent staining

After anesthesia, transcardial perfusion with 0.1 mol/L PBS was performed, followed by perfusion with 4% paraformaldehyde (pH 7.4). The cerebral hemispheres were removed and placed in 4% paraformaldehyde for post-fixation for 24 h. After that, the brains were dehydrated with 30% sucrose in PBS until they sank to the bottom. Next, the brains were coronally sliced into 10-mm sections, which were fixed on slides and used for immunofluorescence staining, and blocked with 5% goat serum plus 0.1% Triton-X-100 at 20°C. The sections were incubated with primary antibodies as follows: Monoclonal mouse anti-Iba1 antibody (1:200, ab15690; Abcam, Cambridge, MA, United States); polyclonal rabbit anti-MANF antibody (1:500, PA5-20432; Thermo Fisher Scientific); polyclonal rabbit anti-iNOS antibody (1:200, ab15323; Abcam); and polyclonal rabbit anti-Arg1 antibody (1:200, ab91279; Abcam) overnight at 4°C. Sections were washed and incubated for 2 h at 20°C with secondary antibodies: Alexa-Fluor-488-conjugated goat anti-mouse IgG (1:200, ab150117; Abcam) and Alexa-Fluor-647-conjugated goat anti-rabbit IgG (1:200, ab150079; Abcam). The nuclei of cells were stained with 4'6-diamidino-2-phenylindole (DAPI; Sigma–Aldrich). The proportion of positive cells was counted in five randomly selected fields from four sections of each brain sample, and the average was calculated. The images were taken under a fluorescent microscope (DP73; Olympus, Tokyo, Japan).

For immunocytochemistry analysis, cells were permeabilized for 15 min with 0.1% Triton X-100 in PBS and blocked for 1 h with PBS containing 0.1% Triton X-100, 2% bovine serum albumin, and 5% goat serum. Cells were incubated overnight with monoclonal mouse anti-Iba1 antibody (1:1000, ab15690; Abcam); polyclonal rabbit anti-MANF antibody (1:1000, PA5-20432; Thermo Fisher Scientific); polyclonal rabbit anti-iNOS antibody (1:1000, ab15323; Abcam); or polyclonal rabbit anti-Arg1 antibody (1:1000, ab91279; Abcam) at 4°C with gentle shaking, followed by 1-h incubation with Alexa-Fluor-488-conjugated goat anti-mouse IgG (1:1000, ab150117; Abcam) or Alexa-Fluor-488-conjugated goat anti-rabbit IgG (1:1000, ab150077; Abcam). Five pictures of each sample were taken by fluorescent microscopy, and the proportions of positive cells were counted.

Western blot analysis

Western blot was used to estimate expression of PDGF-AA/MANF and UPR-associated proteins. Rat brain tissues or cultured cells were homogenized in a commercially available buffer (RIPA Lysis Buffer, Strong; GenStar Biosolutions Co. Ltd., Beijing, China), with added dithiothreitol, phenylmethylsulfonyl fluoride, and protease inhibitor cocktail (Beyotime Biotechnology Co. Ltd., Shanghai, China). The homogenates were centrifuged at 14000 rpm for 15 min at 4°C. The supernatants were collected and protein concentrations were tested with a commercially available kit (BCA Protein Assay Kit; Beyotime Biotechnology). The samples were stored at -80°C until assay and were thawed only once. The cerebral samples or cell extracts were subjected to SDS-PAGE and transferred to polyvinyldifluoridine membranes (Millipore). The blocked membranes were incubated at 4°C overnight with primary antibodies. The primary antibodies were: Polyclonal rabbit anti-MANF antibody (1:500, PA5-20432; Thermo Fisher Scientific); polyclonal rabbit anti-PDGF-AA antibody (1:500, ab216619; Abcam); polyclonal rabbit anti-XBP1 antibody (1:1000, ab37152; Abcam); polyclonal rabbit anti-ATF6 antibody (1:1000, ab203119; Abcam); and monoclonal rabbit anti-glyceraldehyde-3-phosphate dehydrogenase (GAPDH)

antibody (1:1000, 5174; Cell Signaling Technology, Danvers, MA, United States). After rinsing, the membranes were incubated for 2 h at 20°C with horseradish-peroxidase-conjugated anti-rabbit antibody (1:10000, 5151; Cell Signaling Technology). Protein was detected using the chemiDocXRS+ chemiluminescence imaging system (Bio-Rad, Hercules, CA, United States), and the density of the bands was determined with Image Lab image acquisition and analysis software (Bio-Rad).

Real-time quantitative reverse transcription-polymerase chain reaction
Total RNA was extracted from rat brain tissues, BMSCs, and microglia by using TRIzol reagent (Invitrogen), and 5 μg of RNA was reverse transcribed with Revert Aid-M0MulV Reverse Transcriptase (MBI Fermentas, Vilnius, Lithuania). A 20-μL reaction with Golden HS SYBR Green qPCR Mix (HaiGene, Harbin, China) was used to perform real-time quantitative reverse transcription-polymerase chain reaction (qRT-PCR) on Bio-Rad Min-Opticon2 (Bio-Rad). All primers used in this study were obtained from Invitrogen. Primer sequences are listed in Table 1. Thermal cycling conditions were 10 min at 95°C and 40 cycles of 15 s at 95°C and 1 min at 60°C. Melt curves were performed upon completion of the cycles to ensure specificity of the product amplification. The expression of target mRNA was shown relative to the levels of GAPDH or U6, normalized to the control. The quantification of the genes of interest was calculated based on ΔΔCT and depicted as $2^{-\Delta\Delta CT}$.

Enzyme-linked immunosorbent assay
As a secretory neurotrophic factor, the secretion of MANF in culture medium of BMSCs was determined with an enzyme-linked immunosorbent assay (ELISA) kit (SAB, College Park, MD, United States). Standard curve and sample concentrations were calculated based on the mean of triplicate measurements for each sample.

Statistical analysis
Statistical analyses were performed with GraphPad Prism for Windows version 7 (San Diego, CA, United States), and the data are presented as the mean ± standard deviation (SD). All data were evaluated for normality by Kolmogorov–Smirnov test. The homogeneity of variance was confirmed using Bartlett's test before applying parametric tests to assess the null hypotheses ($P > 0.05$). Two-way analysis of variance (ANOVA) with Bonferroni *post hoc* test was performed for statistical analysis of mNSS and Bederson's score. The other comparisons between each group for statistical significance were performed by one-way ANOVA with Tukey's *post hoc* test for more than two groups. $P < 0.05$ was considered statistically significant.

RESULTS

In vitro construction of genetically modified BMSCs
The morphological features of the BMSCs were observed at passage 3 (Figure 2A). BMSCs were analyzed by flow cytometry, which showed that they were positive for cell surface antigens, CD90 and CD73, and negative for CD11b and CD45 (Figure 2B). We determined by ELISA whether BMSCs secrete MANF. After cell transfection and G418 (600 μg/mL) selection, qRT-PCR and Western blot showed that the BMSCs-siMANF2 group expressed the lowest MANF mRNA (Figure 2C) and protein (Figure 2D) levels in comparison with other groups. MANF secretion in the BMSCs-siMANF2 group was significantly decreased compared with that in the control and BMSCs-NC groups (Figure 2E). Thus, the BMSCs-siMANF2 group was used for further experiments. These results demonstrated that we have successfully developed the genetically modified BMSCs to downregulate MANF for subsequent cell transplantation.

Transplantation of BMSCs enhances functional outcomes and decreases infarction volume via production of MANF after 7 d in stroke rats
Similar to our previous experiments[39], intrastriatal BMSCs transplantation in I/R injury rats significantly improved neurological function compared to that in I/R and I/R + PBS groups. The mNSS and Bederson's score were increased in the I/R + BMSCs-siMANF group compared to those in the I/R + BMSCs and I/R + BMSCs-NC groups. However, both scores of the I/R + BMSCs-siMANF group were significantly lower than those of the I/R and I/R+PBS groups (Figure 3A and B). In line with the results of neurological function tests, TTC staining of rat brain slices further

Table 1 Primers used for real-time quantitative reverse transcription polymerase chain reaction analysis		
Gene	Forward primer (5'–3')	Reverse primer (5'–3')
MANF	TCCGCTACTGTAAGCAAGGT	CTTCACCTAGGATCTTGGTG
PDGF-AA	GCCATTCCCGCAGTTTG	GGCTGGCACTTGACGCT
XBP1	ATGTTTTTCAAATGTCCTTCCCCAG	TGACAGAGAAAGGGAGGCTGGTAAG
ATF6	TGCAGGTGTATTACGCTTCGC	GCAGGTGATCCCTTCGAAATG
iNOS	ATCCCGAAACGCTACACTT	CGGCTGGACTTCTCACTC
Arg1	CAGTGGCGTTGACCTTGT	TGGTTCTGTTCGGTTTGC
NF-YA	CTGAGACTCCACAGCCATCA	GGATCTTCCCTTCTGCCTCT
NF-YB	CTGGATGGGGCTGACTGTAT	AGGAGGTACGCCAGTCTGTG
NF-YC	ACCCTTGCATGGCACTAAAG	GCTGGATGGTGGTCGTAGAA
*miR-30a**	CTTTCAGTCGGATGTTTGC	GTGCGTGTCGTGGAGTCG
GAPDH	GCAAGTTCAACGGCACAG	GCCAGTAGACTCCACGACAT
U6	CTCGCTTCGGCAGCACA	AACGCTTCACGAATTTGCGT

MANF: Mesencephalic astrocyte–derived neurotrophic factor; *PDGF-AA*: Platelet-derived growth factor-AA; *XBP1*: X-box binding protein 1; *ATF6*: Activating transcription factor 6; *iNOS*: Inducible nitric oxide synthase; *Arg-1*: Arginase-1; *NF-Y*: Nuclear factor-Y; *GAPDH*: Glyceraldehyde-3-phosphate dehydrogenase.

demonstrated that cerebral infarct volume of the I/R + BMSCs-siMANF group was significantly larger compared with that in the BMSCs and BMSCs-NC treated rats on day 7 after cerebral I/R injury (Figure 3D). BMSCs treatment enhanced functional recovery and ameliorated cerebral ischemic damage in the acute cerebral I/R injury period by secreting MANF.

MANF secreted by BMSCs induces MANF expression in ischemic brains

MANF was induced at the early stage of cerebral ischemia. Infusion of BMSCs significantly increased MANF levels in the I/R and I/R + PBS groups at 24 h after MCAO. MANF protein and mRNA levels in the I/R + BMSCs-siMANF group were significantly decreased in comparison with those in the I/R + BMSCs and I/R + BMSCs-NC groups, but BMSCs-siMANF treatment totally attenuated the increased MANF levels in the ischemic brains (Figure 4A and B). It is known that MANF is expressed in microglia/macrophages and other central nervous system cells or infiltrating immune cells. The results of Western blot and qRT-PCR therefore reflected the changes in MANF in brain tissues of mixed cell types. To test whether BMSC treatment affects MANF expression in microglia/macrophages, we also detected MANF in the cells using immunofluorescent double staining with anti-MANF and anti-Iba1, a marker of microglia/macrophages. Unlike low expression of MANF⁺/Iba1⁺ in the sham group, increased numbers of MANF⁺/Iba1⁺ cells were detected in the I/R and I/R + PBS groups, suggesting that ER stress was involved in ischemia-induced activation of microglia/macrophages. BMSC treatment further elevated expression of MANF⁺/Iba1⁺ cells compared with that in the I/R and I/R + PBS groups. Consistent with Western blot and qRT-PCR results, there were significantly fewer MANF⁺/Iba1⁺ cells in the I/R + BMSCs-siMANF group than in the I/R + BMSCs and I/R + BMSCs-NC groups (Figure 4C). These results suggested that the beneficial effects of BMSCs might not be restricted to paracrine actions but might be due to their induction of host microglia/macrophages to produce MANF.

### BMSCs-mediated MANF paracrine signaling upregulates MANF expression in microglia

The purity of our primary microglia culture was assessed by immunocytochemical staining with Iba1, being expressed by > 98% of the cells (Figure 5A). To test whether BMSCs affects expression of MANF in microglia, Transwell cocultures of microglia with BMSCs were established. LPS treatment significantly increased protein and mRNA levels of MANF in microglia, and these were significantly enhanced after coculture with BMSCs. In the LPS + BMSCs-siMANF group, BMSCs-induced MANF expression was significantly reduced, but not completely eliminated (Figure 5B and C).
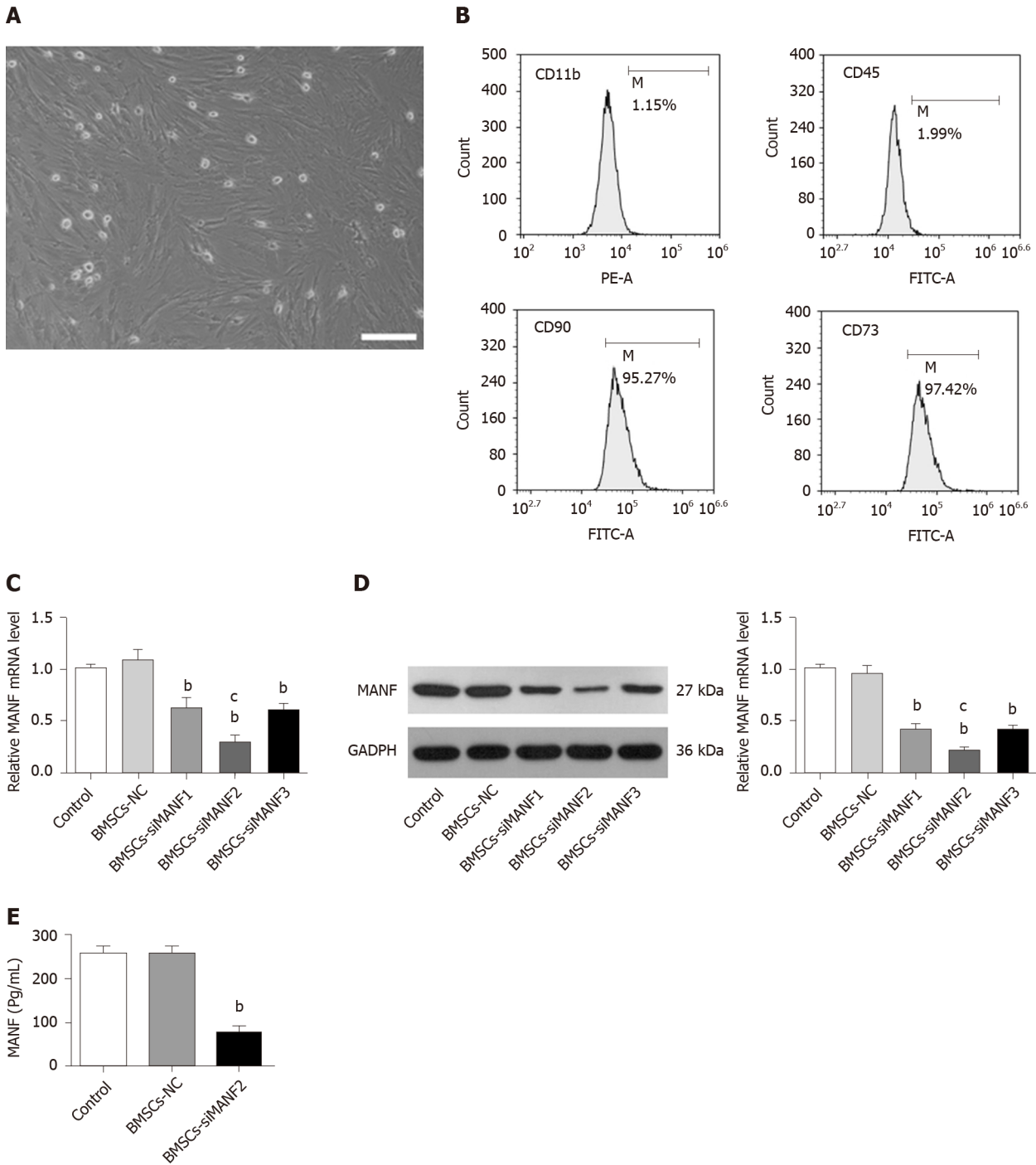
Figure 2 Construction of genetically modified bone marrow mesenchymal stem cells. A: Cultured bone marrow mesenchymal stem cells (BMSCs) were homogeneous in size and morphology. Scale bar = 500 μm; B: Flow cytometry for detection of BMSCs surface markers; C and D: qRT-PCR (C) and Western blot analysis (D) of MANF levels in BMSCs transfected with MANF-siRNA or NC. E: ELISA of MANF in culture medium of BMSCs. $^bP < 0.01$ *vs* Control and BMSCs-NC groups; $^cP < 0.05$ *vs* BMSCs-siMNAF1 and BMSCs-siMANF3 groups. The values are expressed as the mean ± SD (*n*=6). MANF: Mesencephalic astrocyte–derived neurotrophic factor; GAPDH: Glyceraldehyde-3-phosphate dehydrogenase; BMSCs: Bone marrow mesenchymal stem cells; BMSCs-NC: Negative control-transfected BMSCs; BMSCs-siMANF: MANF siRNA-transfected BMSCs.

Accordingly, immunofluorescence showed that more MANF⁺ microglia were found in the LPS and LPS + vehicle groups compared with the control group. Additionally, the number of MANF⁺ microglia was further increased after coculture with BMSCs. However, in the LPS + BMSCs-siMANF group, there were significantly fewer MANF⁺ microglia than in the LPS + BMSCs and LPS + BMSCs-NC groups (Figure 5D). These results demonstrated that the expression of microglia-derived MANF was activated by MANF secreted from BMSCs. We then tested whether MANF secreted from BMSCs regulates the levels of XBP1 mRNA and miR-30a*. As a key transcription factor of MANF, XBP1 mRNA expression was markedly upregulated in the activated microglia,
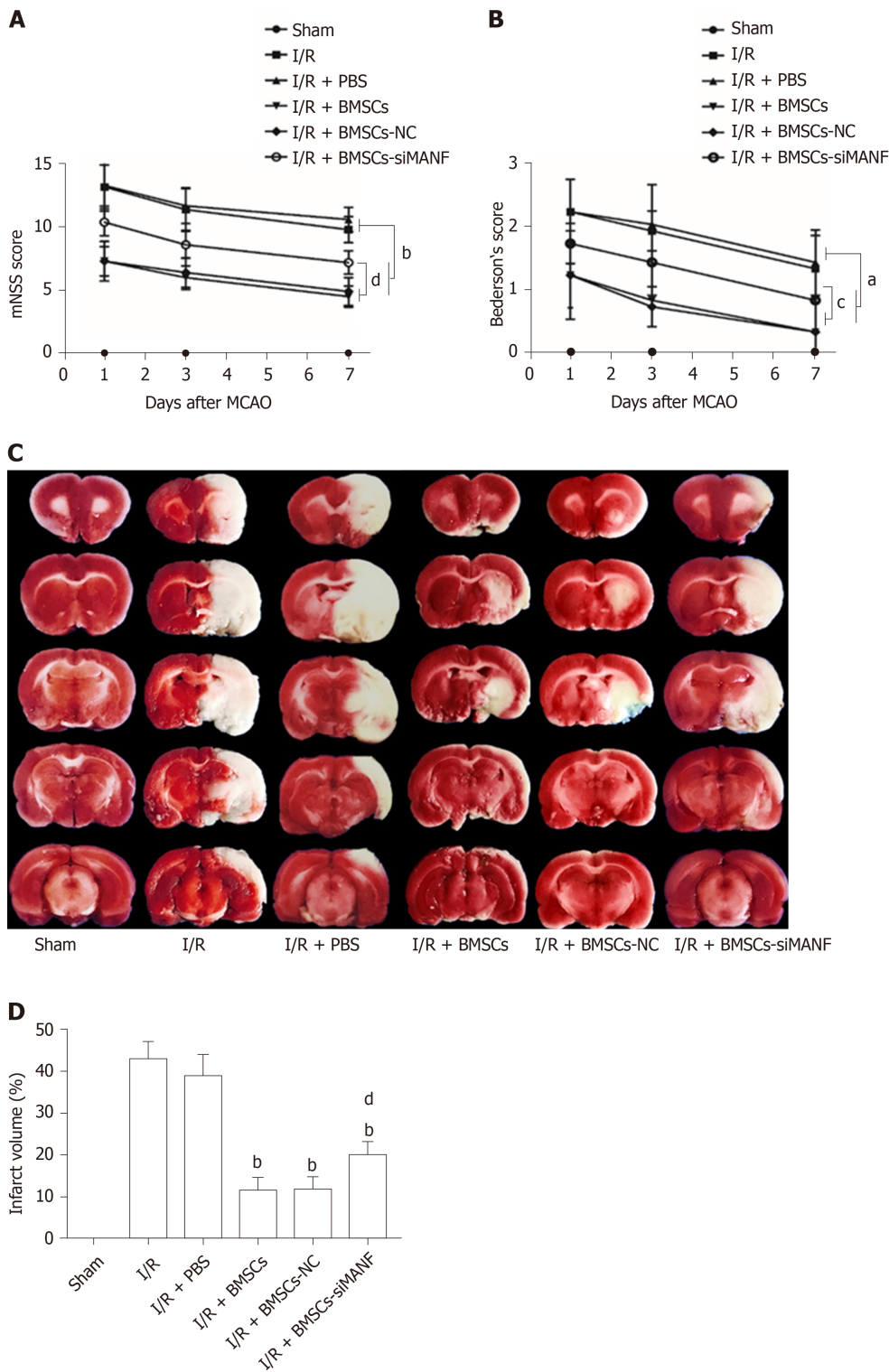
Figure 3 Effects of mesencephalic astrocyte–derived neurotrophic factor on post-stroke recovery and infarction volume in cerebral I/R rats treated with bone marrow mesenchymal stem cells. A and B: mNSS (A) and Bederson's (B) score evaluation of the behavior of rats on days 1, 3, and 7 after MCAO surgery; C and D: TTC staining (C) and quantitative analysis (D) of lesion volume on day 7 post-stroke. [a]$P < 0.05$, [b]$P < 0.01$ *vs* I/R and I/R + PBS groups; [c]$P < 0.05$, [d]$P < 0.01$ *vs* I/R + BMSCs and I/R + BMSCs-NC groups. The values are expressed as the mean ± SD (*n* =10). MANF: Mesencephalic astrocyte–derived neurotrophic factor; mNSS: Modified neurological severity scores; I/R: Ischemia/reperfusion; MCAO: Middle cerebral artery occlusion; PBS: Phosphate-buffered saline; BMSCs: Bone marrow mesenchymal stem cells; BMSCs-NC: Negative control-transfected BMSCs; BMSCs-siMANF: MANF siRNA-transfected BMSCs.

and BMSCs induced further enhancement of gene expression (Supplement Figure 1A). As a shown in Supplement Figure 1B, miR-30a* level was downregulated in LPS-induced microglial cells, and further decreased after coculture with BMSCs. There was no difference in the levels of XBP1 mRNA and miR-30a* in the LPS + BMSCs-siMANF
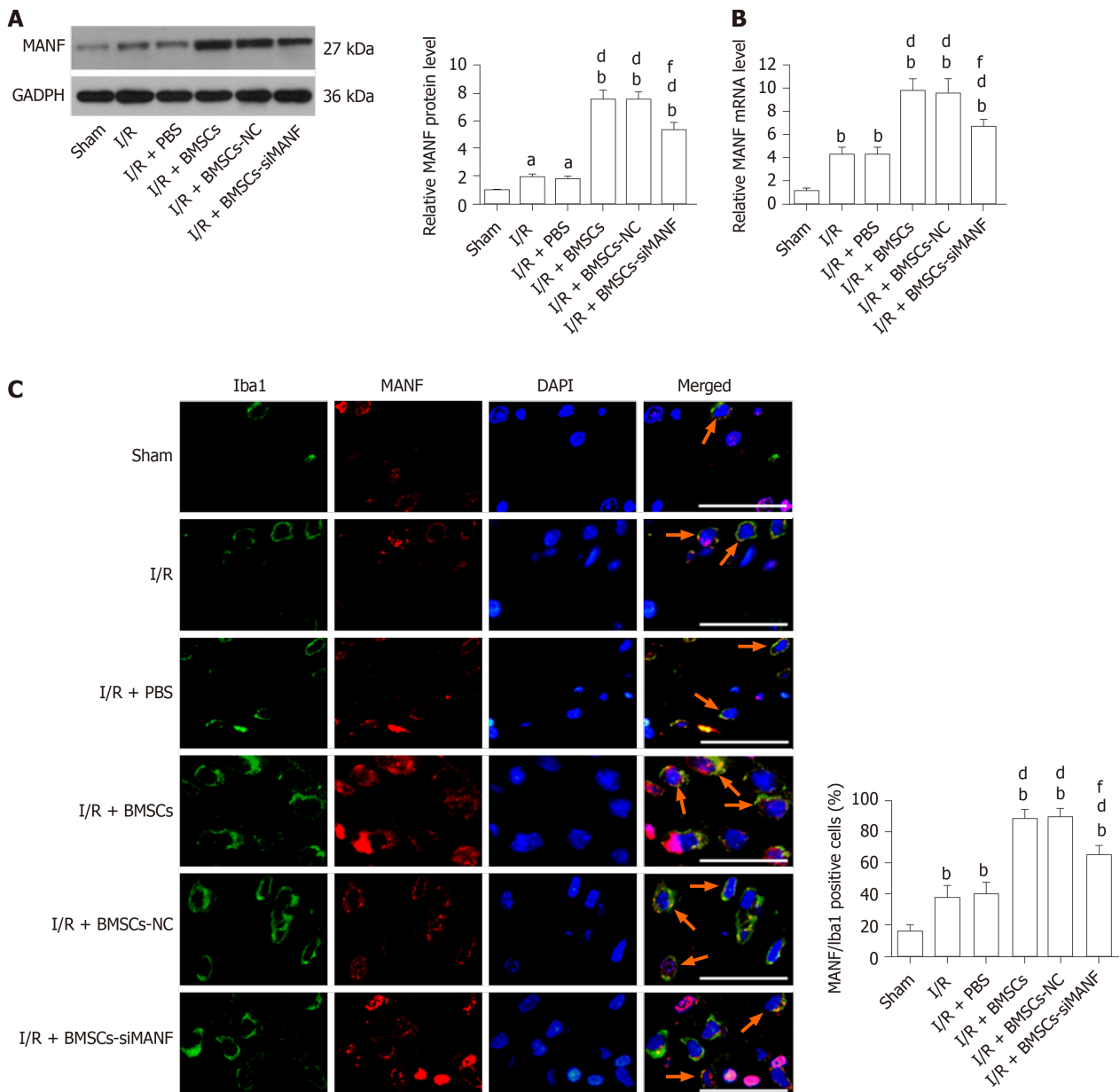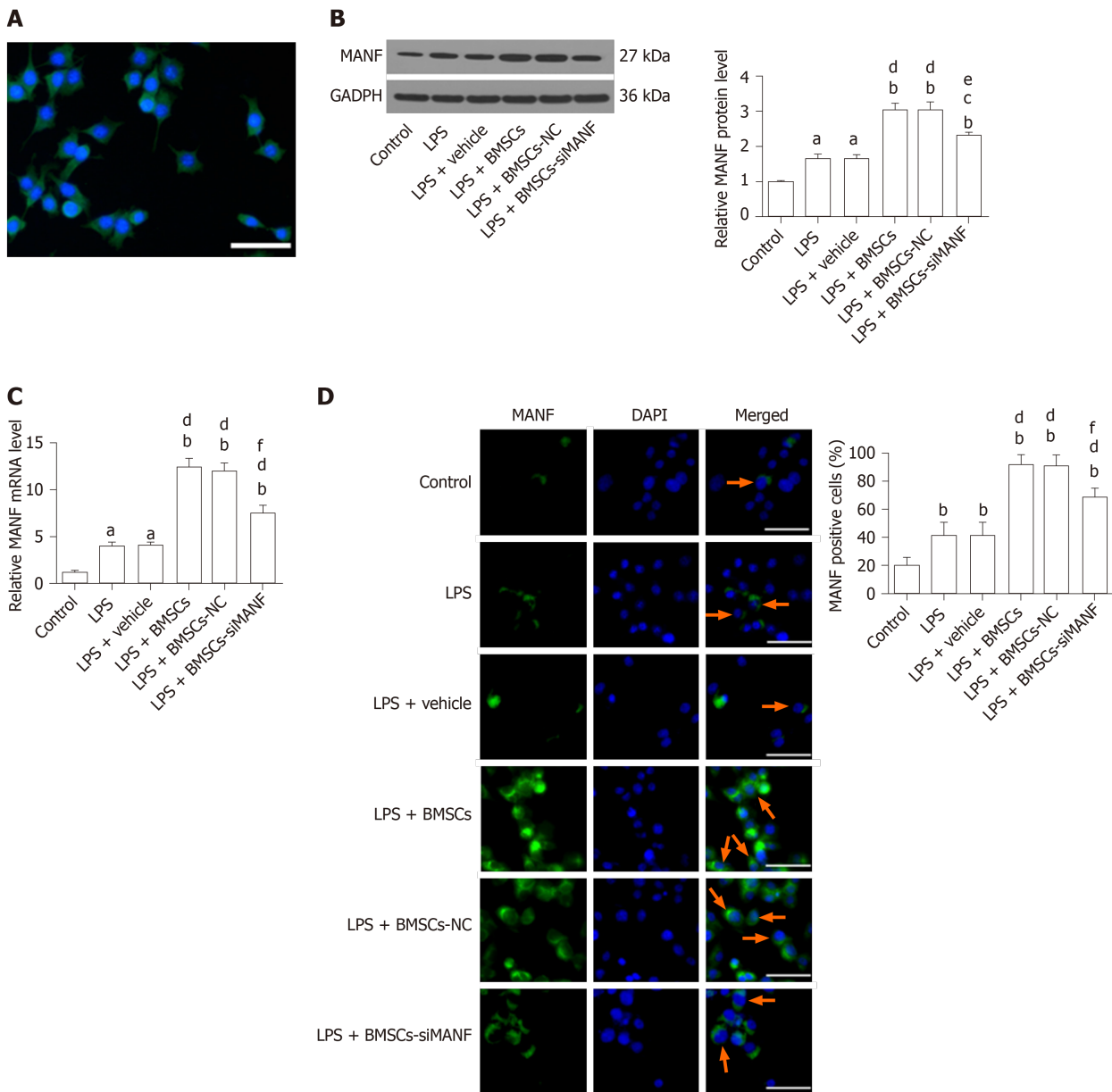
Figure 4 Mesencephalic astrocyte–derived neurotrophic factor expression in microglia/macrophages in cerebral ischemia. A and B: Western blot (A) and qRT-PCR analysis (B) of MANF expression at 24 h after cerebral I/R injury; C: Immunohistochemical analysis of MANF expression in the microglia/macrophages of the injured brains. Representative images of immunohistochemical staining for the microglia/macrophage marker Iba1 (green) and MANF (red), with DAPI (blue) as a nuclear counterstain, are shown. [a]$P < 0.05$, [b]$P < 0.01$ *vs* Sham group; [d]$P < 0.01$ *vs* I/R and I/R + PBS groups; [f]$P < 0.01$ *vs* I/R + BMSCs and I/R + BMSCs-NC groups. Scale bar = 50 μm. Arrows point to the MANF[+]/Iba1^{+} cells. The values are expressed as the mean ± SD (*n* = 6). MANF: Mesencephalic astrocyte–derived neurotrophic factor; GAPDH: Glyceraldehyde-3-phosphate dehydrogenase; I/R: Ischemia/reperfusion; PBS: Phosphate-buffered saline; BMSCs: Bone marrow mesenchymal stem cells; BMSCs-NC: Negative control-transfected BMSCs; BMSCs-siMANF: MANF siRNA-transfected BMSCs; Iba1: Ionized calcium-binding adapter molecule; DAPI: 4'6-diamidino-2-phenylindole.

group compared to those in the LPS + BMSCs-NC and LPS + BMSCs groups. These results suggested that MANF did not affect the transcriptional levels of XBP1 and miR-30a*, and some soluble factors might regulate miR-30a*/XBP1 expression.

MANF secreted from BMSCs promotes M2 phenotype microglia/macrophages in ischemic brains

To test whether MANF plays an important role in BMSCs-induced M2 polarization, we evaluated the phenotypes of activated microglia/macrophages. Ischemia significantly increased the number of iNOS[+]/Iba1^{+} cells and iNOS mRNA expression at 24 h after I/R injury, while BMSCs significantly lowered both levels. iNOS expression in the I/R + BMSCs-siMANF group was significantly increased compared with that in the I/R + BMSCs and I/R + BMSCs-NC groups (Figure 6A and B). In

Figure 5 Mesencephalic astrocyte–derived neurotrophic factor expression in lipopolysaccharide-stimulated microglia. A: Representative immunocytochemical staining for Iba1 (green) and co-staining for DAPI (blue) as a nuclear counterstain. Scale bar = 50 μm; B–D: Western blot (B), qRT-PCR (C), and immunocytochemistry analysis (D) of MANF expression in microglia pretreated with 100 ng/mL LPS for 24 h with or without BMSCs. Representative images of MANF (green), with DAPI (blue) as a nuclear counterstain, are shown. [a]P < 0.05, [b]P < 0.01 *vs* Control group; [c]P < 0.05, [d]P < 0.01 *vs* LPS and LPS + vehicle groups; [e] P < 0.05, [f]P < 0.01 *vs* LPS + BMSCs and LPS + BMSCs-NC groups. Scale bar = 50 μm. Arrows point to the MANF^{+} cells. The values are expressed as the mean ± SD (*n* = 6). MANF: Mesencephalic astrocyte–derived neurotrophic factor; GAPDH: Glyceraldehyde-3-phosphate dehydrogenase; LPS: Lipopolysaccharide; BMSCs: Bone marrow mesenchymal stem cells; BMSCs-NC: Negative control-transfected BMSCs; BMSCs-siMANF: MANF siRNA-transfected BMSCs; DAPI: 4'6-diamidino-2-phenylindole.

contrast, ischemia increased the percentage of Arg1^{+}/Iba1^{+} cells, and Arg1 mRNA levels were significantly enhanced by BMSCs infusion. The effect of BMSC-induced Arg1 expression was attenuated after BMSCs-siMANF transplantation (Figure 6C and D). The data indicated that the mechanism of BMSC-induced M2 polarization was related to the effect of secreted MANF on microglia/macrophages, leading to M2 phenotype after ischemic stroke.

### MANF secreted from BMSCs induces microglia polarization to M2 phenotype

To identify the potential molecular mechanism underlying BMSC-induced M2 microglia, immunocytochemical staining and qRT-PCR were performed for iNOS and Arg1. Resting microglia did not express iNOS, and LPS upregulated iNOS expression. LPS-induced iNOS mRNA and protein expression was markedly decreased by coculture with BMSCs (Figure 7A and B). In contrast, untreated microglia expressed

A

B

C
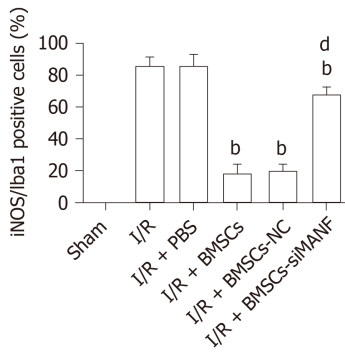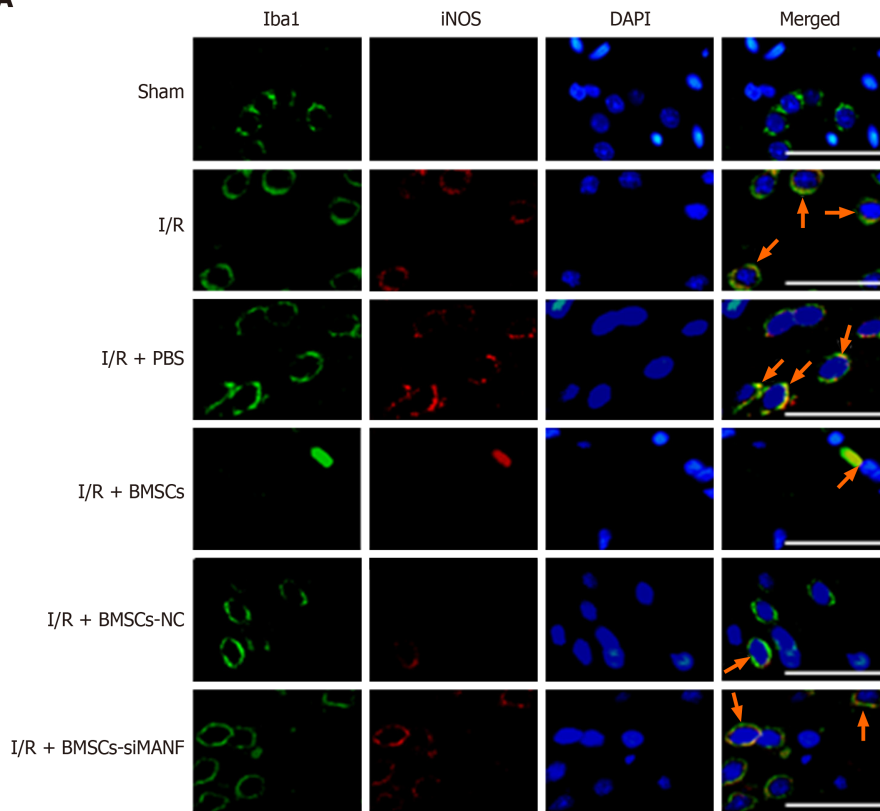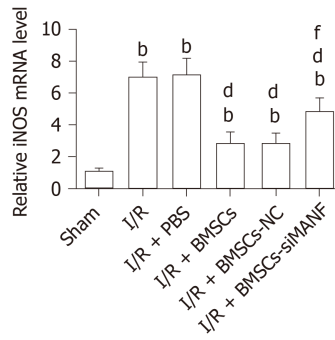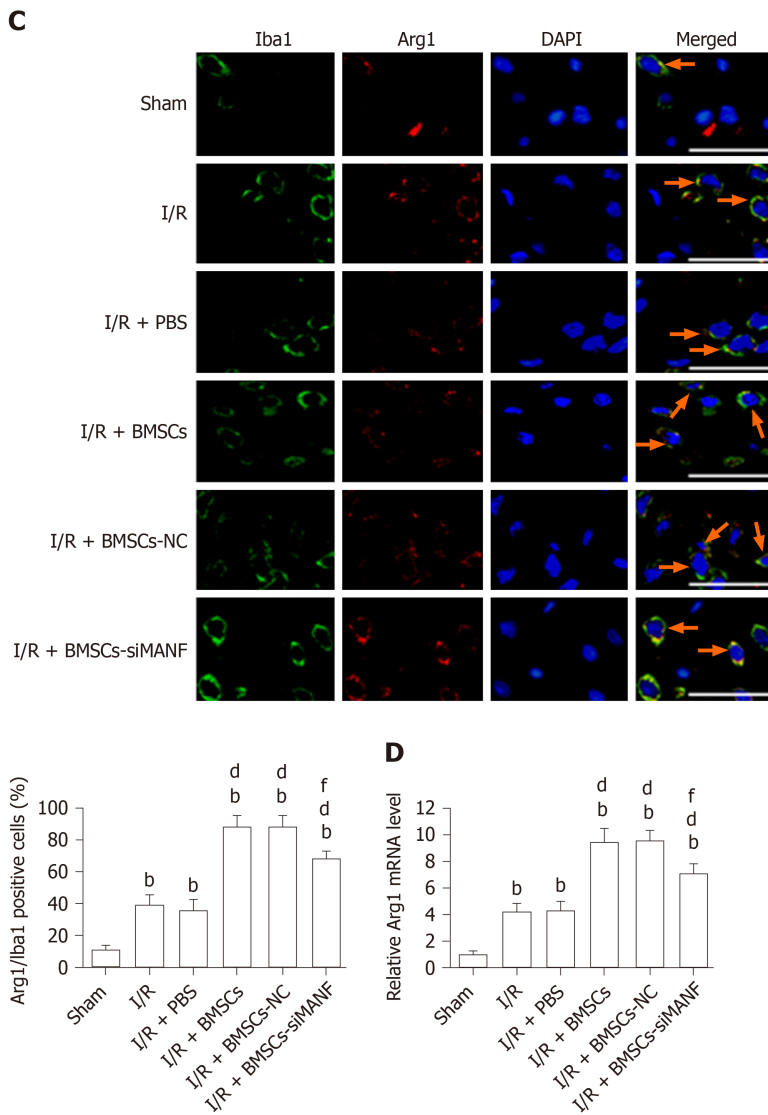
Figure 6 *In vivo* analysis of M1 and M2 polarization markers after cerebral I/R injury with bone marrow mesenchymal stem cell treatment.
A: Immunohistochemistry analysis of iNOS expression in the microglia/macrophages of the ischemic brain after 24 h of MCAO. Representative images of the indicated brain double stained with Iba1 (green) and iNOS (red), with DAPI (blue) as a nuclear counterstain, are shown. [b]*P* < 0.01 *vs* I/R and I/R + PBS groups; [d]*P* < 0.01 *vs* I/R + BMSCs and I/R + BMSCs-NC groups. Scale bar = 50 μm. Arrows point to the iNOS[+]/Iba1^{+} cells; B: qRT-PCR analysis of iNOS expression in acute ischemic stroke rat brains; C: Immunohistochemical analysis of Arg1 expression in the microglia/macrophages of ischemic brains. Representative images of the indicated brain double stained with Iba1 (green) and Arg1 (red), with DAPI (blue) as a nuclear counterstain, are shown. Scale bar = 50 μm. Arrows point to the Arg1^{+}/Iba1^{+} cells; D: qRT-PCR analysis of Arg1 expression in rat brains at 24 h after MCAO. [b]*P* < 0.01 *vs* Sham group; [d]*P* < 0.01 *vs* I/R and I/R + PBS groups; [f]*P* < 0.01 *vs* I/R + BMSCs and I/R + BMSCs-NC groups. The values are expressed as the mean ± SD (*n* = 6). I/R: Ischemia/reperfusion; PBS: Phosphate-buffered saline; BMSCs: Bone marrow mesenchymal stem cells; BMSCs-NC: Negative control-transfected BMSCs; BMSCs-siMANF: MANF siRNA-transfected BMSCs; iNOS: Inducible nitric oxide synthase; Arg-1: Arginase-1; Iba1: Ionized calcium-binding adapter molecule; DAPI: 4'6-diamidino-2-phenylindole.

low levels of Arg1, and LPS stimulation reduced Arg1 expression in microglia. Expression of Arg1 was induced at mRNA and protein levels in LPS-stimulated microglia cocultured with BMSCs (Figure 7C and D). In addition, compared to coculture with BMSCs and BMSCs-NC, BMSCs-siMANF partially attenuated Arg1 or enhanced iNOS expression in microglial cells. Supporting the findings described *in vivo*, these results showed that BMSCs released MANF, thus resulting in the shift from M1 to M2 phenotype.

MiR-30a* targets XBP1 in microglia

XBP1 is a potential target of the miR-30* family, and overexpression of miR-30a* caused a significant decrease in XBP1 expression, with greater effect than the other miR-30* family members[33]. Therefore, to identify the roles for endogenous miR-30a* in XBP1 expression in microglia, HAPI cells were transfected with miR-mimics, miR-NC, anti-miR, or anti-NC. qRT-PCR and Western blot showed that cells transfected with miR-mimics showed a significant decrease in expression of XBP1, while

A

B
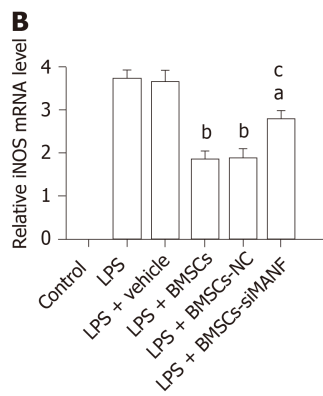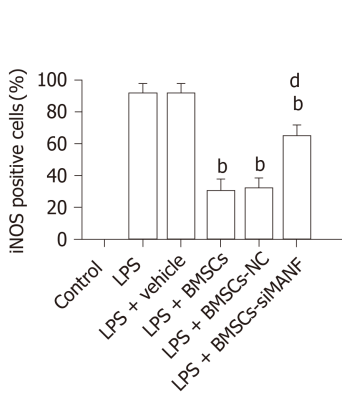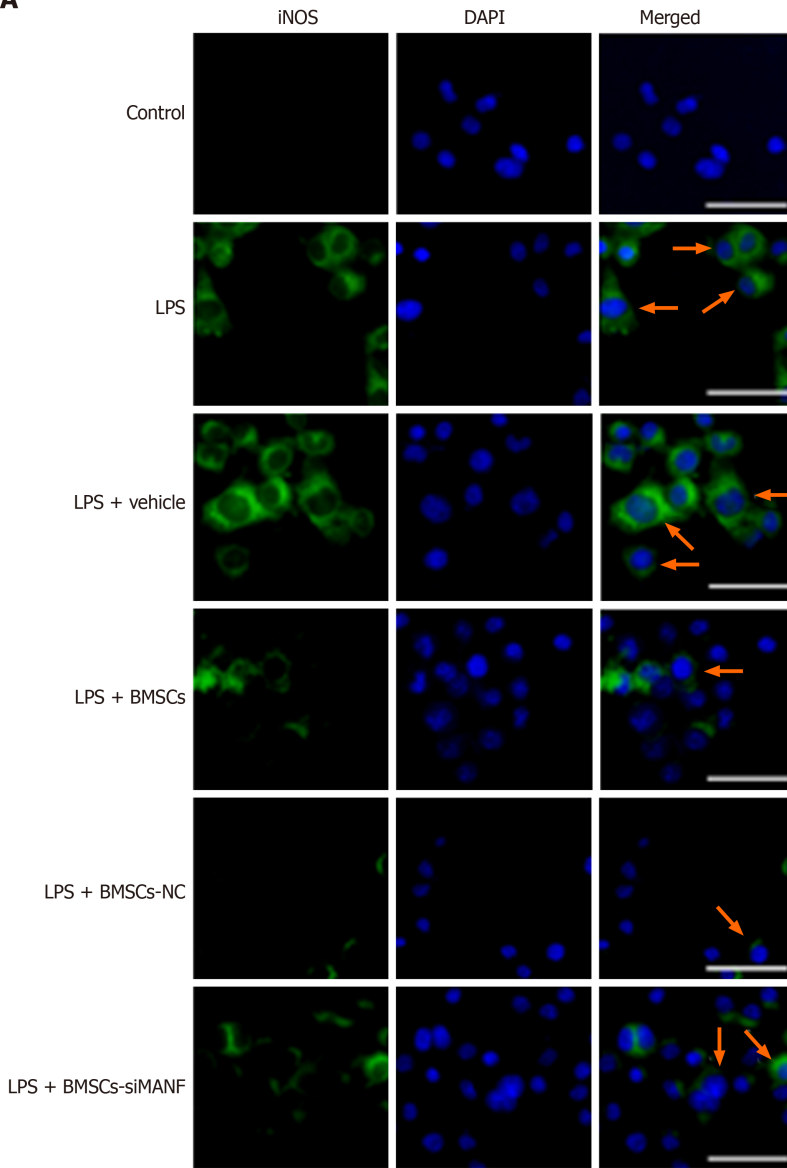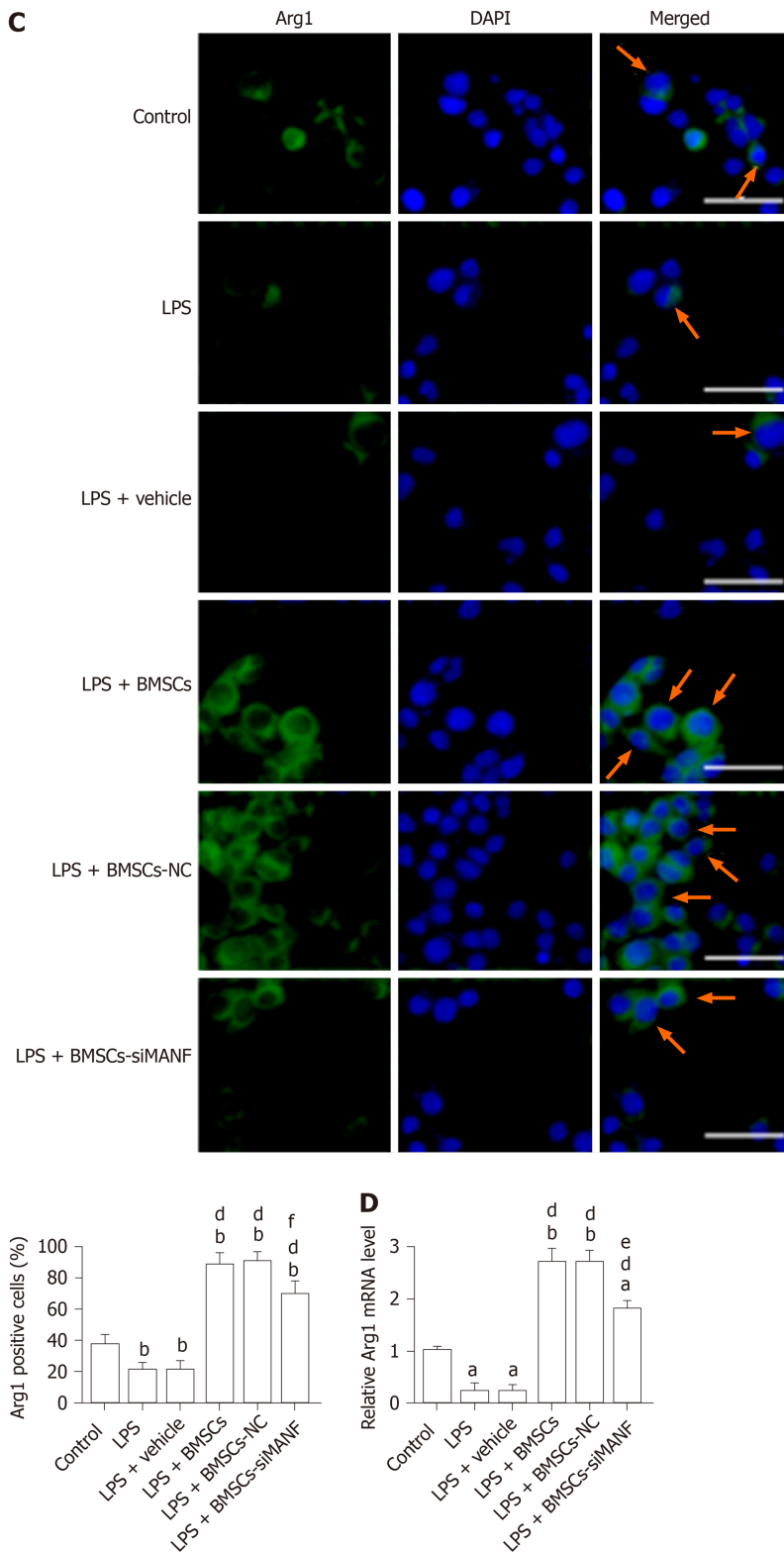
Figure 7 ***In vitro* analysis of M1 and M2 polarization markers following exposure to lipopolysaccharide and bone marrow mesenchymal stem cells.** A and B: Immunocytochemistry (A) and qRT-PCR analysis (B) of iNOS expression in microglia. Representative images of immunofluorescence staining for iNOS (green), with DAPI (blue) as a nuclear counterstain, are shown. [a]$P < 0.05$, [b]$P < 0.01$ *vs* LPS and LPS + vehicle groups; [c]$P < 0.05$, [d]$P < 0.01$ *vs* LPS + BMSCs and LPS+BMSCs-NC groups. Scale bar = 50 μm. Arrows point to the iNOS^{+} cells; C and D: Immunocytochemistry (C) and qRT-PCR analysis (D) of Arg1 expression in LPS-stimulated microglia in the presence or absence of BMSCs. Representative images of immunofluorescence staining for Arg1 (green), with DAPI (blue) as a nuclear counterstain, are shown. [a]$P < 0.05$, [b]$P < 0.01$, *vs* Control group; [d]$P < 0.001$ *vs* LPS and LPS + vehicle groups; [e]$P < 0.05$, [f]$P < 0.01$ *vs* LPS + BMSCs and LPS+BMSCs-NC groups. Scale bar = 50 μm. Arrows point to the Arg1^{+} cells. The values are expressed as the mean ± SD (n = 6). LPS: Lipopolysaccharide; BMSCs: Bone marrow mesenchymal stem cells; BMSCs-NC: Negative control-transfected BMSCs; BMSCs-siMANF: MANF siRNA-transfected BMSCs; iNOS: Inducible nitric oxide synthase; Arg-1: Arginase-1; DAPI: 4'6-diamidino-2-phenylindole.

inhibition of endogenous miR-30a* by synthetic anti-miR resulted in upregulation of

XBP1 (Figure 8A and B). In contrast, MANF expression required ATF6 or XBP1. These transcription factors recognize ERSE and ERSE-II in the presence of the nuclear factor-Y (NF-Y, a heterotrimer of NF-YA, NF-YB, and NF-YC subunits)[40]. Therefore, to investigate whether miR-30a* targets other transcription factors besides XBP1, we performed qRT-PCR to analyze mRNA levels in HAPI cells. However, the ATF6 and NF-YA–C expression did not significantly change in any group (Figure 8C and D). These results suggested that miR-30a* inhibited expression of XBP1, targeting neither ATF6 nor NF-YA–C mRNA in microglia.

PDGF-AA causes XBP1 and MANF upregulation by inhibiting miR-30a* expression

We next sought to determine whether exogenous PDGF-AA attenuates expression of miR-30a* and thereby leads to an increased level of XBP1 and MANF. To assess the effect of PDGF-AA-induced MANF expression, various concentrations of PDGF-AA were evaluated. As shown by Western blot (Figure 9A), 0.1, 1, and 10 ng/mL of PDGF-AA significantly affected MANF expression in LPS-stimulated HAPI cells. Although PDGF-AA at lower concentrations of 0.1 and 1 ng/mL also significantly promoted MANF expression, 10 ng/mL of PDGF-AA revealed a greater effect. Thus, 10 ng/mL of PDGF-AA was used for further studies. There was a more significant decrease in miR-30a* expression in LPS-treated cells, and further downregulation after PDGF-AA treatment (Figure 9B). Transfection of miR-mimics reversed the suppressive effect of PDGF-AA on miR-30a* expression. As expected, ATF6, XBP1, and their downstream target MANF were significantly increased in LPS-induced ER stress processes of HAPI cells. PDGF-AA treatment did not influence ATF6 expression (Figure 9C and D). In contrast, protein and mRNA expression of XBP1 and MANF was further induced by10 ng/mL of PDGF-AA. Overexpression of miR-30a* in HAPI cells attenuated induction of XBP1 (Figure 9E and F) and MANF (Figure 9G and H) in response to PDGF-AA, but it did not completely reduce XBP1 expression. These results suggested that the PDGF-AA/XBP1/MANF signaling pathway was, at least in part, mediated by miR-30a*.

MANF secreted by BMSCs does not influence PDGF-AA expression in ischemic brains or in microglia

We determined whether MANF paracrine signaling mediated by BMSCs affects expression of PDGF-AA *in vivo* and *in vitro*. We found that PDGF-AA expression was upregulated at 24 h after brain ischemia. Although BMSCs promoted PDGF-AA expression, its protein and mRNA levels in the I/R + BMSCs-siMANF group did not show significant differences compared with those in the BMSCs and BMSCs-NC groups (Figure 10A and B). Similar to what we found *in vivo*, LPS-stimulated microglia produced a higher amount of PDGF-AA compared with the resting cells. Exposure to BMSCs significantly upregulated PDGF-AA expression in microglial cells, whereas the levels of PDGF-AA in the LPS + BMSCs-siMANF group were unchanged in comparison to those in the LPS+BMSCs-NC and LPS+BMSCs groups (Figure 10C and D). These findings allowed us to devise a new signaling pathway: BMSCs-secreted PDGF-AA and MANF synergistically increased MANF expression in the activated microglia. In addition, we provided evidence that PDGF-AA enhanced XBP1 expression *via* miR-30a* downregulation, resulting in MANF upregulation, finally leading to M2 polarization (Figure 10E).

DISCUSSION

In this study, we reported for the first time the contribution of MANF in BMSCs-induced M2 phenotype polarization as well as in the functional outcomes after stroke. Importantly, the *in vitro* study confirmed that BMSCs drove M2 microglia polarization through MANF secretion. We also studied the mechanisms underlying the PDGF-AA/MANF signaling pathway and found that PDGF-AA enhanced XBP1 expression by miR-30a* downregulation, leading to increased MANF expression in response to ER stress in the activated microglia.

Ischemic injury to the brain involves activation and mobilization of microglia and recruited macrophages, followed by coordinated balance of M1 and M2 phenotypes. M2-like microglia/macrophages can suppress inflammation and promote neuronal network recovery through tissue remodeling by growth factors, cytokines, and proteinases[41]. Inflammatory and regenerative responses are tightly co-regulated during tissue repair, and the proinflammatory microenvironments negatively affect integration and repair[42,43]. Strategy switching of the cerebral environment from a proinflammatory toxic to an anti-inflammatory and neuroprotective condition could
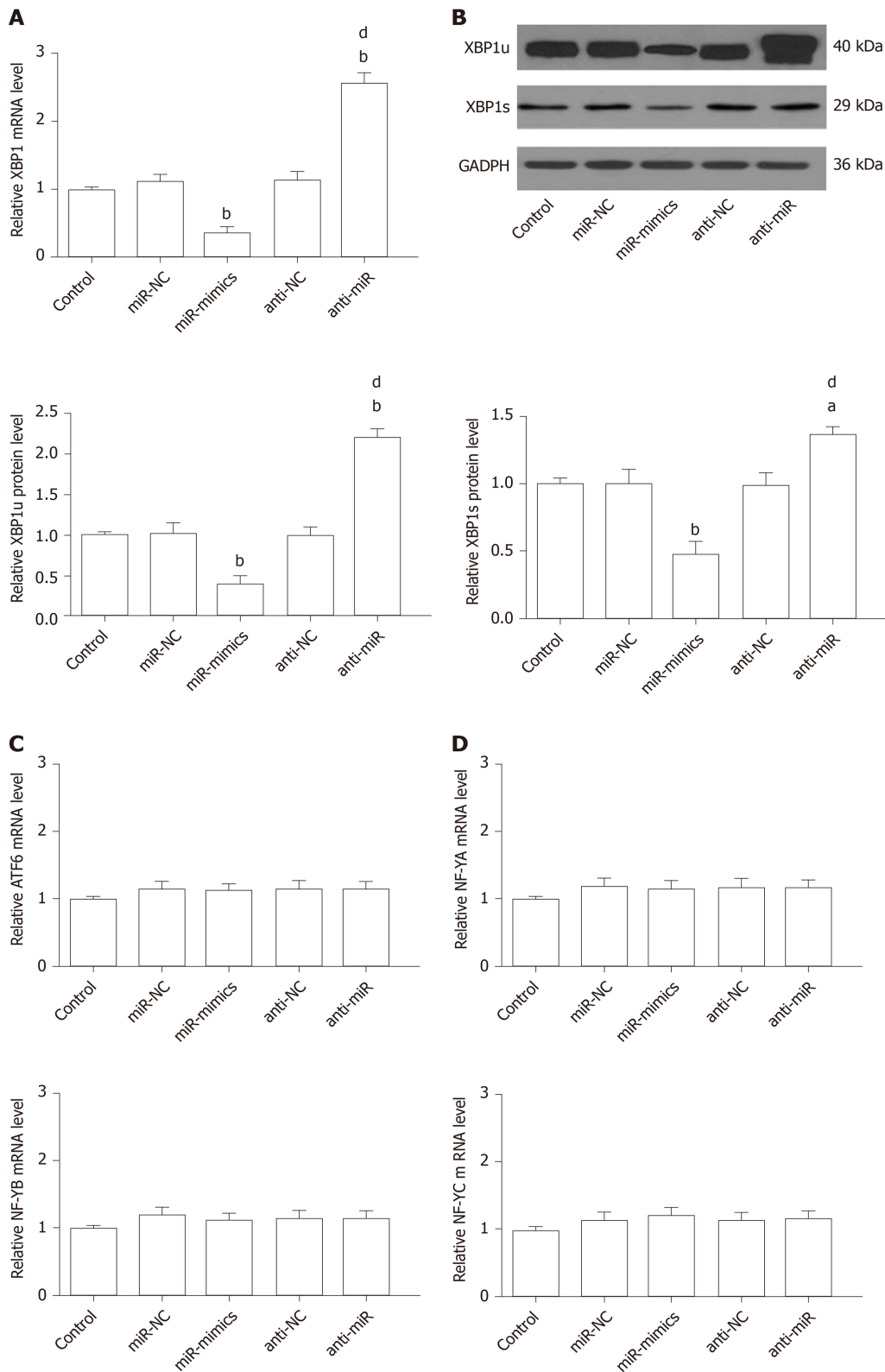
Figure 8 miR-30a* inhibits X-box binding protein 1 expression without regulating the levels of activating transcription factor 6 and NF-YA–C in HAPI cells. A and B: qRT-PCR (A) and Western blot analysis (B) of XBP1 expression in HAPI cells transfected with miR-mimics, anti-miR, or corresponding NC oligonucleotides; C and D: qRT-PCR analysis of ATF6 (C) and NF-YA–C (D) expression in HAPI cells after transfection of miR-mimics, anti-miR, or corresponding NC oligonucleotides. [a]$P < 0.05$, [b]$P < 0.01$ *vs* Control, miR-NC and anti-NC groups; [d]$P < 0.01$ *vs* miR-mimics group. The values are expressed as the mean ± SD ($n = 6$). XBP1: X-box binding protein 1; GAPDH: Glyceraldehyde-3-phosphate dehydrogenase; ATF6: Activating transcription factor 6; NF-Y (A,B,C): Nuclear factor-Y (A,B,C); miR-NC: miR-30a*-negative control-transfected microglia; miR-mimics: miR-30a*-mimics-transfected microglia; anti-NC: anti-miR-30a*-negative control-transfected microglia; anti-miR: miR-30a*-inhibitor-transfected microglia.

be a potential therapy for ischemic stroke. BMSCs therapy is the desired approach for addressing this issue. Therefore, BMSCs-regulated microglia/macrophage polarization
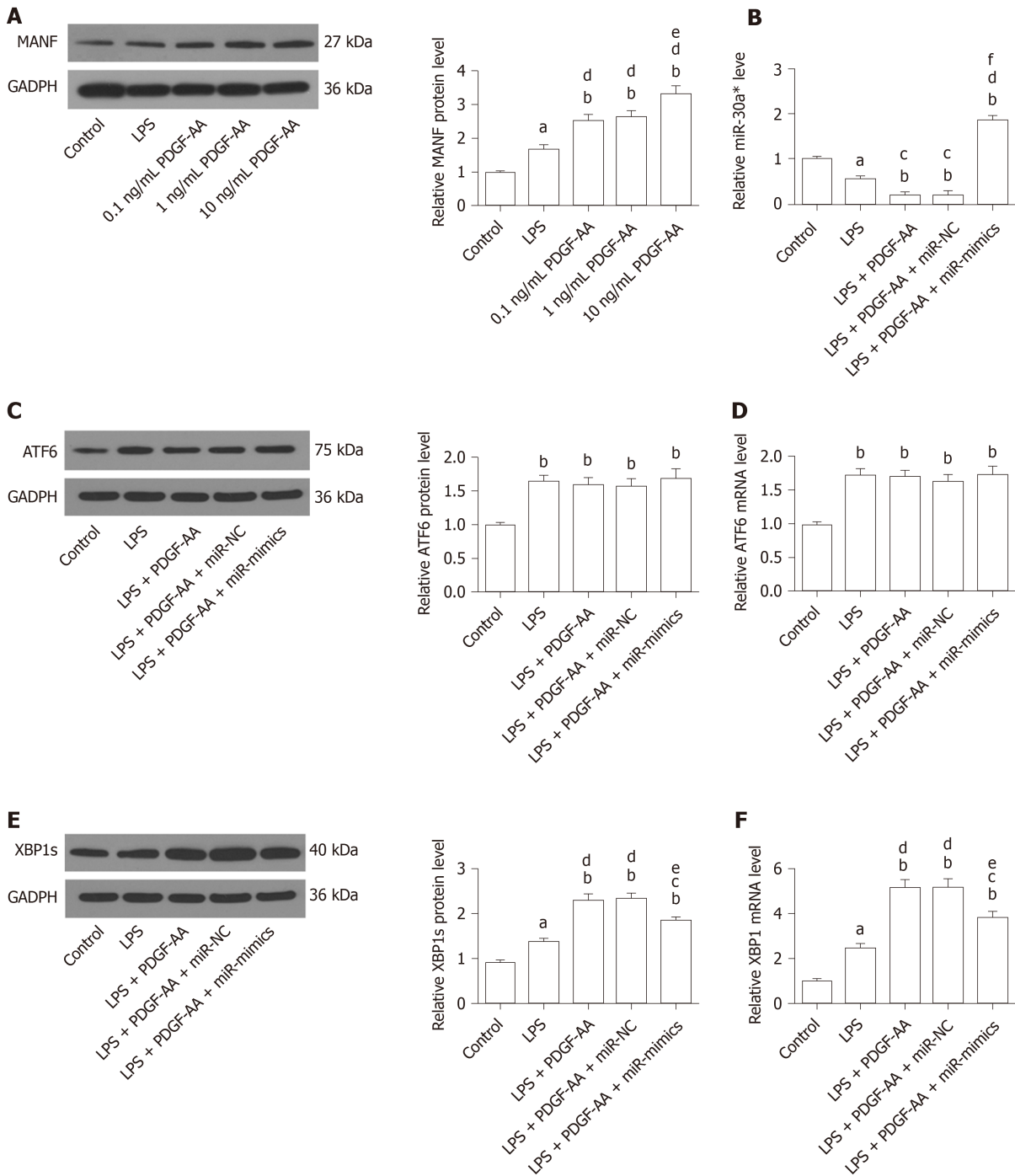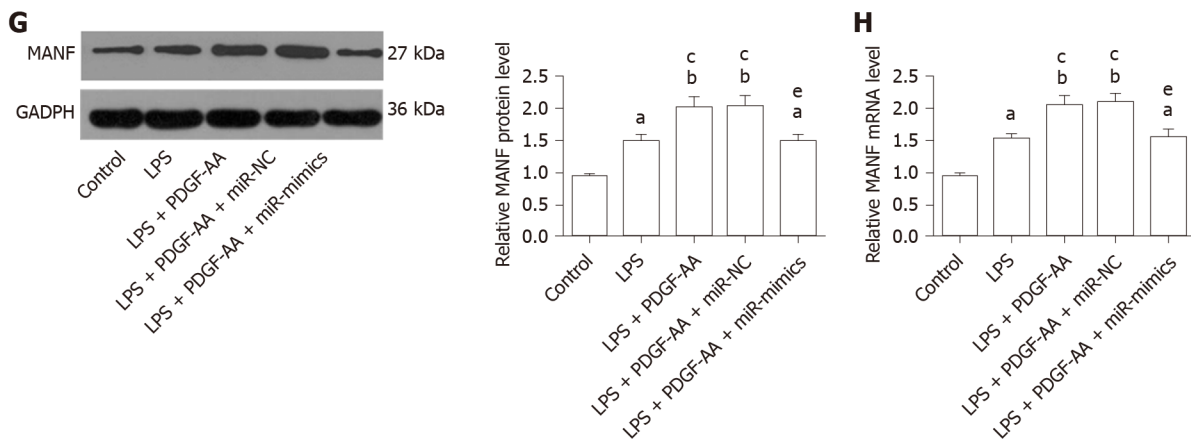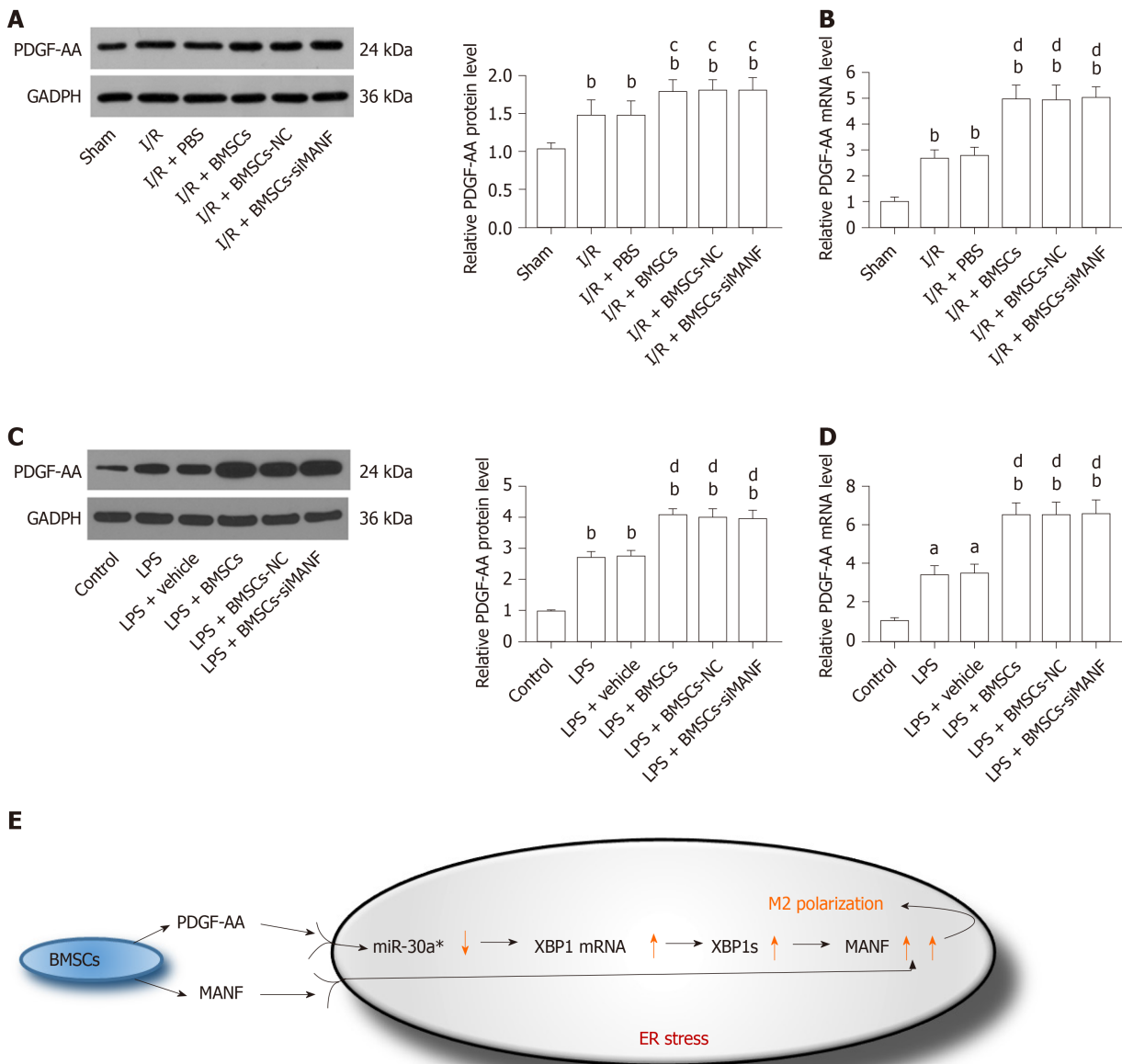
Figure 9 Platelet-derived growth factor-AA-mediated induction of mesencephalic astrocyte–derived neurotrophic factor involves miR-30a*/X-box binding protein 1 signaling in HAPI cells stimulated by lipopolysaccharide. A: Western blot analysis of PDGF-AA-induced MANF expression in activated HAPI cells. [a]$P < 0.05$, [b]$P < 0.01$ *vs* Control group; [d]$P < 0.01$ *vs* LPS group; [e]$P < 0.05$ *vs* 0.1 ng/mL and 1 ng/mL PDGF-AA groups; B: qRT-PCR analysis of miR-30a* expression in untreated or 10 ng/mL PDGF-AA-treated activated HAPI cells transfected with or without miR-mimics or miR-NC; C and D: Western blot (C) and qRT-PCR analysis (D) of ATF6 expression in untreated or 10 ng/mL PDGF-AA-treated activated HAPI cells transfected with or without miR-mimics or miR-NC; E and F: Western blot (E) and qRT-PCR analysis (F) of XBP1 expression in untreated or 10 ng/mL PDGF-AA-treated activated HAPI cells transfected with or without miR-mimics or miR-NC; G and H: Western blot (G) and qRT-PCR analysis (H) of MANF expression in untreated or 10 ng/mL PDGF-AA-treated activated HAPI cells transfected with or without miR-mimics or miR-NC. [a]$P < 0.05$, [b]$P < 0.01$ *vs* Control group; [c]$P < 0.05$, [d]$P < 0.01$ *vs* LPS group; [e]$P < 0.05$, [f]$P < 0.01$ *vs* LPS + PDGF-AA and LPS + PDGF-AA + miR-NC groups. The values are expressed as the mean ± SD ($n = 6$). MANF: Mesencephalic astrocyte–derived neurotrophic factor; PDGF-AA: Platelet-derived growth factor-AA; XBP1: X-box binding protein 1; ATF6: Activating transcription factor 6; GAPDH: Glyceraldehyde-3-phosphate dehydrogenase; LPS: Lipopolysaccharide; miR-NC: miR-30a*-negative control-transfected microglia; miR-mimics: miR-30a*-mimics-transfected microglia.

is crucial for transplantation of stem cells after cerebral ischemia.

Although MANF was initially discovered by its neurotrophic activity, further studies revealed that MANF could have an immunomodulatory effect on macrophage differentiation in the retina and spleen[29,44]. Our recent study has demonstrated that the therapeutic effects on stroke are probably related to the paracrine function of BMSCs[45]. Due to the anti-inflammatory property of MANF, a secretory neurotrophic factor, we constructed genetically modified BMSCs as vehicles that downregulated MANF expression for this cell transplantation in MCAO rats. In earlier studies, MANF was shown to be induced at the early stage of brain ischemia, decreasing to the control level at 1 wk after ischemia[17,46]. The protein levels of MANF started to increase at 3 h, and peaked at 24 h in a rat model of intracerebral or subarachnoid hemorrhage[47,48]. These results indicated that MANF was induced by ER stress in a time-dependent manner. Therefore, as the time point for exploring the role of MANF in BMSCs-mediated M2 polarization, 24 h of reperfusion after 2 h of ischemia was reasonable. M1 phenotype macrophages express high levels of iNOS that compete with Arg1 for L-arginine, the common substrate of both enzymes. Switching the L-arginine metabolism from iNOS to Arg1 is vital to limit NO production and downregulate inflammation[49]. Thus, iNOS and Arg1 represent the classical M1 and M2 phenotypes, respectively. Temporal analysis of cell phenotypes in ischemic animals has demonstrated that microglia/macrophages respond dynamically to ischemic injury, experiencing an early healthy M2 phenotype, followed by a transition to a sick M1 phenotype[5]. In keeping with time-dependent MANF expression in a rat brain ischemia model, MANF might play a critical role in the M2-to-M1 shift, highlighting the importance of BMSCs transplantation at the early stage of ischemic stroke. Previous studies have demonstrated that MANF expression is upregulated in the activated microglial cells, without investigating whether and how MANF modulates microglia polarization[50]. In this study, we found that MANF released from BMSCs acted directly on microglial cells and macrophages, which functioned both as sources and targets of MANF. Importantly, we observed that MANF secreted by BMSCs directly induced M2 microglia/macrophage polarization, which explained the mechanism of BMSCs-induced immunomodulatory effects. Although we performed the short-term behavioral tests in the MCAO rats, our data showed that BMSCs treatment promoted functional recovery and decreased the infarct volume caused by MCAO *via* production of MANF. Therefore, the cytoprotective and M2-inducible functions of MANF paracrine signaling are likely to synergize to promote tissue recovery. Meanwhile, we noted that MANF had overlap with DAPI, suggesting that MANF localizes in the

Figure 10 *In vivo* and *in vitro* analysis of platelet-derived growth factor-AA expression. A and B: Western blot (A) and qRT-PCR analysis (B) of PDGF-AA expression in the injured brains. [b]$P < 0.01$ *vs* Sham group; [c]$P < 0.05$, [d]$P < 0.01$ *vs* I/R and I/R + PBS groups; C and D: Western blot (C) and qRT-PCR analysis (D) of PDGF-AA in LPS-stimulated microglia in the presence or absence of BMSCs. [a]$P < 0.05$, [b]$P < 0.01$ *vs* Control group; [d]$P < 0.01$ *vs* LPS and LPS + vehicle groups. The values are expressed as the mean ± SD ($n = 6$); E: Proposed mechanism for synergistic regulation of PDGF-AA/miR-30a*/XBP1/MANF pathway and MANF paracrine signaling during BMSCs-induced M2 polarization. PDGF-AA: Platelet-derived growth factor-AA; GAPDH: Glyceraldehyde-3-phosphate dehydrogenase; I/R: Ischemia/reperfusion; LPS: Lipopolysaccharide; PBS: Phosphate-buffered saline; BMSCs: Bone marrow mesenchymal stem cells; BMSCs-NC: Negative control-transfected BMSCs; BMSCs-siMANF: MANF siRNA-transfected BMSCs; XBP1: X-box binding protein 1; MANF: Mesencephalic astrocyte–derived neurotrophic factor; ER: Endoplasmic reticulum.

nucleus and focal ischemia induced its relocalization, which indicated that MANF might be a negative regulator of inflammation and mediate the crosstalk with the nuclear factor (NF)-κB pathway[51]. In contrast, LPS-induced MANF expression was localized in the cytoplasm, whereas nuclear MANF immunopositive signals were not observed. The reason why MANF exhibits different cellular distribution under different pathological conditions is worthy of further investigation.

In this study, inhibition of MANF significantly decreased, but did not eliminate, the effect of BMSCs on microglia/macrophage polarization. To explore other soluble mediators responsible for interactions between BMSCs and microglia/macrophages, the PDGF-AA/MANF axis was investigated. We illustrated a clear dose-responsive effect of PDGF-AA on induction of MANF in microglia. The maximal induction dose of PDGF-AA was 10 ng/mL, however, low concentrations of PDGF-AA could enhance MANF expression as well. There is growing evidence supporting the concept that secretion of PDGF-AA, but not -AB and -BB ligand, by BMSCs promotes M2

polarization and neurorestoration in MCAO rats[11]. Although we were unable to determine the PDGF-AA/MANF signaling pathway *in vivo*, we speculate that the indirect (induction of MANF expression in microglia/macrophages) activity of PDGF-AA contributes to its tissue repair effect against ischemic injury. Meanwhile, we found that reduction of MANF secreted by BMSCs did not influence PDGF-AA expression, suggesting that the molecular mechanism of BMSC-mediated activation of PDGF-AA expression involves some other soluble factors, at least not the downstream signaling pathways of MANF. In addition, as a transcription factor, XBP1 activation plays a key role in the UPR, which has been proven to recognize and bind to ERSE and ERSE-II, whereas both exert different effects on MANF transcription in mice and humans[26,52]. A previous study has shown that MANF may in turn regulate the function of XBP1s at the protein level in the UPR, but does not affect the transcriptional levels of XBP1[19], which is in accordance with our study. In this investigation, PDGF-AA treatment significantly increased expression of XBP1s protein and XBP1 mRNA, but not ATF6 in LPS-induced ER stress processes of microglia. Therefore, having a key role in promoting MANF expression, XBP1 is the downstream target of PDGF-AA.

A few ER-stress-inducible miRNAs have been identified and shown to negatively regulate translation of certain secretory pathway proteins, suggesting that miRNAs play integral roles in the UPR[53,54]. Recently, miR-30a has been reported to be an important regulator of the inflammatory response in microglia[55]. To clarify whether miR-30a* has similar effects to miR-30a, we further established the essential roles of miR-30a* in XBP1 expression in microglia. Our results revealed that miR-30a* was downregulated and this downregulation increased XBP1 expression, resulting in upregulation of MANF in the LPS-induced microglia. Importantly, we found that PDGF-AA treatment decreased miR-30a* expression, leading to the enhanced expression of XBP1 and its downstream target MANF. A recent study confirmed that NF-κB played a critical role in upregulating expression of miR-30c-2* in UPR[32]. Based on this, we cannot exclude the possibility that MANF-induced activity of PDGF-AA partially contributes to its inhibitory effect against the NF-κB/miR-30a* pathway, so how PDGF-AA influences miR-30a* expression deserves further study.

To our knowledge, this is the first study to demonstrate that BMSCs can induce M2 phenotype microglia *via* a novel secreted factor, MANF, both *in vivo* and *in vitro*. We noticed a synergistic relation between PDGF-AA and MANF secreted by BMSCs, which led to upregulation of MANF in microglia that then promoted M2 polarization. Our data provide a link between a miRNA and direct regulation of the ER stress response and reveal a novel molecular mechanism by which the PDGF-AA pathway, *via* miR-30a*, influences XBP1-mediated MANF expression in the UPR. To date, the receptor and the signaling pathway for MANF are still obscure[56], although protein kinase C signaling has been activated downstream of MANF[57]. Therefore, how MANF functions in a paracrine manner to induce M2 polarization needs further attention and investigation.

In conclusion, our present study demonstrated that the paracrine function of MANF may contribute to the mechanisms underlying BMSCs-derived M2 microglia/macrophage polarization. As a paracrine interaction between BMSCs and microglia through synergistic effect of MANF and PDGF-AA pathway governing M2 polarization, PDGF-AA/miR-30a*/XBP1/MANF signaling for MANF induction should be taken into account.

ARTICLE HIGHLIGHTS

Research background
Bone marrow mesenchymal stem cells (BMSCs) have been widely studied for their applications in stem-cell-based stroke therapy. Although anti-inflammatory and paracrine effects of grafted BMSCs have been shown, the precise mechanism underlying BMSCs-induced M2 microglia polarization remains unclear. Mesencephalic astrocyte-derived neurotrophic factor (MANF) is a new member of the neurotrophic factor families, which is upregulated during endoplasmic reticulum (ER) stress and protects several cell populations from ER-stress-induced cell death *in vivo* or *in vitro*.

Research motivation
MANF and platelet-derived growth factor (PDGF)-AA/MANF signaling have been shown to have an immunoregulatory effect on M1/M2 macrophage differentiation to

promote damage repair and neuroprotective effect.

Research objectives

In the present study, the aim was to detect whether MANF paracrine signaling mediated BMSCs-induced M2 polarization and to determine the molecular mechanism underlying the PDGF-AA/MANF signaling pathway.

Research methods

We first identified the secretion of MANF by BMSCs and developed genetically modified BMSCs that downregulated MANF expression. BMSCs were injected into the right striatum 24 h before cerebral ischemia/reperfusion injury. Using a rat middle cerebral artery occlusion (MCAO) model and BMSCs/microglia Transwell coculture system, the effect of BMSCs-mediated MANF paracrine signaling on M1/M2 polarization *in vivo* and *in vitro* was determined by Western blot, quantitative reverse transcription-polymerase chain reaction (qRT-PCR), and immunofluo-rescence. The transgenic microglia were used to assess the effect of miR-30a* on PDGF-AA/miR-30a*/X-box binding protein (XBP) 1/MANF signaling pathway. Western blot and qRT-PCR were conducted to examine the expression of ER stress-related markers.

Research results

In vivo or *in vitro*, BMSCs induced functional recovery and increased M2 marker expression, as well as decreased expression of M1 marker, which were inhibited by MANF siRNA treatment. As another soluble factor secreted by BMSCs, PDGF-AA upregulated XBP1 and MANF expression *via* downregulating miR-30a* in the activated microglia.

Research conclusions

BMSCs promote M2 phenotype polarization through MANF secretion, which might partially contribute to the functional outcomes in stroke rats. Besides MANF paracrine signaling, the PDGF-AA/miR-30a*/XBP1/MANF signaling pathway influences BMSCs-mediated M2 polarization.

Research perspectives

These findings will be beneficial in development of an approach with high efficiency to regulate BMSCs-induced M2 polarization, and strengthen the potential of cell therapeutics to enhance the reversal of behavioral deficits caused by ischemic stroke.

REFERENCES

1   **Donnan GA**, Fisher M, Macleod M, Davis SM. Stroke. *Lancet* 2008; **371**: 1612-1623 [PMID: 18468545 DOI: 10.1016/S0140-6736(08)60694-7]

2   **Yang Z**, Zhu L, Li F, Wang J, Wan H, Pan Y. Bone marrow stromal cells as a therapeutic treatment for ischemic stroke. *Neurosci Bull* 2014; **30**: 524-534 [PMID: 24817388 DOI: 10.1007/s12264-013-1431-y]

3   **Wan H**, Li F, Zhu L, Wang J, Yang Z, Pan Y. Update on therapeutic mechanism for bone marrow stromal cells in ischemic stroke. *J Mol Neurosci* 2014; **52**: 177-185 [PMID: 24048741 DOI: 10.1007/s12031-013-0119-0]

4   **Wang C**, Li F, Guan Y, Zhu L, Fei Y, Zhang J, Pan Y. Bone marrow stromal cells combined with oxiracetam influences the expression of B-cell lymphoma 2 in rats with ischemic stroke. *J Stroke Cerebrovasc Dis* 2014; **23**: 2591-2597 [PMID: 25267587 DOI: 10.1016/j.jstrokecerebrovasdis.2014.05.035]

5   **Hu X**, Li P, Guo Y, Wang H, Leak RK, Chen S, Gao Y, Chen J. Microglia/macrophage polarization dynamics reveal novel mechanism of injury expansion after focal cerebral ischemia. *Stroke* 2012; **43**: 3063-3070 [PMID: 22933588 DOI: 10.1161/STROKEAHA.112.659656]

6   **Xiong XY**, Liu L, Yang QW. Functions and mechanisms of microglia/macrophages in neuroinflammation and neurogenesis after stroke. *Prog Neurobiol* 2016; **142**: 23-44 [PMID: 27166859 DOI: 10.1016/j.pneurobio.2016.05.001]

7   **Chernykh ER**, Shevela EY, Starostina NM, Morozov SA, Davydova MN, Menyaeva EV, Ostanin AA. Safety and Therapeutic Potential of M2 Macrophages in Stroke Treatment. *Cell Transplant* 2016; **25**: 1461-1471 [PMID: 26671426 DOI: 10.3727/096368915X690279]

8   **Hegyi B**, Környei Z, Ferenczi S, Fekete R, Kudlik G, Kovács KJ, Madarász E, Uher F. Regulation of mouse microglia activation and effector functions by bone marrow-derived mesenchymal stem cells. *Stem Cells Dev* 2014; **23**: 2600-2612 [PMID: 24870815 DOI: 10.1089/scd.2014.0088]

9   **Kim J**, Hematti P. Mesenchymal stem cell-educated macrophages: a novel type of alternatively activated macrophages. *Exp Hematol* 2009; **37**: 1445-1453 [PMID: 19772890 DOI: 10.1016/j.exphem.2009.09.004]

10   **Donega V**, Nijboer CH, van Tilborg G, Dijkhuizen RM, Kavelaars A, Heijnen CJ. Intranasally administered mesenchymal stem cells promote a regenerative niche for repair of neonatal ischemic brain injury. *Exp Neurol* 2014; **261**: 53-64 [PMID: 24945601 DOI: 10.1016/j.expneurol.2014.06.009]

11   **Yan T**, Venkat P, Chopp M, Zacharek A, Ning R, Roberts C, Zhang Y, Lu M, Chen J. Neurorestorative Responses to Delayed Human Mesenchymal Stromal Cells Treatment of Stroke in Type 2 Diabetic Rats. *Stroke* 2016; **47**: 2850-2858 [PMID: 27729575 DOI: 10.1161/STROKEAHA.116.014686]

12   **Pan YJ**, Sun RH. Atkinson K. The United States of America and Canada: John Wiley & Sons; 690-713 The potential of bone marrow mesenchymal stromal cells in the treatment of ischemic stroke. In: Atkinson K. The Biology and Therapeutic Application of Mesenchymal Cells. The United States of America and Canada: John Wiley & Sons, 2016: 690-713 [DOI: 10.1002/9781118907474.ch48]

13   **Petrova P**, Raibekas A, Pevsner J, Vigo N, Anafi M, Moore MK, Peaire AE, Shridhar V, Smith DI, Kelly J, Durocher Y, Commissiong JW. MANF: a new mesencephalic, astrocyte-derived neurotrophic factor with selectivity for dopaminergic neurons. *J Mol Neurosci* 2003; **20**: 173-188 [PMID: 12794311 DOI: 10.1385/JMN:20:2:173]

14   **Apostolou A**, Shen Y, Liang Y, Luo J, Fang S. Armet, a UPR-upregulated protein, inhibits cell proliferation and ER stress-induced cell death. *Exp Cell Res* 2008; **314**: 2454-2467 [PMID: 18561914 DOI: 10.1016/j.yexcr.2008.05.001]

15   **Chen YC**, Sundvik M, Rozov S, Priyadarshini M, Panula P. MANF regulates dopaminergic neuron development in larval zebrafish. *Dev Biol* 2012; **370**: 237-249 [PMID: 22898306]

16   **Xu S**, Di Z, He Y, Wang R, Ma Y, Sun R, Li J, Wang T, Shen Y, Fang S, Feng L, Shen Y. Mesencephalic astrocyte-derived neurotrophic factor (MANF) protects against Aβ toxicity via attenuating Aβ-induced endoplasmic reticulum stress. *J Neuroinflammation* 2019; **16**: 35 [PMID: 30760285 DOI: 10.1186/s12974-019-1429-0]

17   **Yu YQ**, Liu LC, Wang FC, Liang Y, Cha DQ, Zhang JJ, Shen YJ, Wang HP, Fang S, Shen YX. Induction profile of MANF/ARMET by cerebral ischemia and its implication for neuron protection. *J Cereb Blood Flow Metab* 2010; **30**: 79-91 [PMID: 19773801 DOI: 10.1038/jcbfm.2009.181]

18   **Mätlik K**, Yu LY, Eesmaa A, Hellman M, Lindholm P, Peränen J, Galli E, Anttila J, Saarma M, Permi P, Airavaara M, Arumäe U. Role of two sequence motifs of mesencephalic astrocyte-derived neurotrophic factor in its survival-promoting activity. *Cell Death Dis* 2015; **6**: e2032 [PMID: 26720341 DOI: 10.1038/cddis.2015.371]

19   **Yang W**, Shen Y, Chen Y, Chen L, Wang L, Wang H, Xu S, Fang S, Fu Y, Yu Y, Shen Y. Mesencephalic astrocyte-derived neurotrophic factor prevents neuron loss via inhibiting ischemia-induced apoptosis. *J Neurol Sci* 2014; **344**: 129-138 [PMID: 25001514 DOI: 10.1016/j.jns.2014.06.042]

20   **Airavaara M**, Chiocco MJ, Howard DB, Zuchowski KL, Peränen J, Liu C, Fang S, Hoffer BJ, Wang Y, Harvey BK. Widespread cortical expression of MANF by AAV serotype 7: localization and protection against ischemic brain injury. *Exp Neurol* 2010; **225**: 104-113 [PMID: 20685313 DOI: 10.1016/j.expneurol.2010.05.020]

21   **Mätlik K**, Anttila JE, Kuan-Yin T, Smolander OP, Pakarinen E, Lehtonen L, Abo-Ramadan U, Lindholm P, Zheng C, Harvey B, Arumäe U, Lindahl M, Airavaara M. Poststroke delivery of MANF promotes functional recovery in rats. *Sci Adv* 2018; **4**: eaap8957 [PMID: 29806020 DOI: 10.1126/sciadv.aap8957]

22   **Hetz C**. The unfolded protein response: controlling cell fate decisions under ER stress and beyond. *Nat Rev Mol Cell Biol* 2012; **13**: 89-102 [PMID: 22251901 DOI: 10.1038/nrm3270]

23   **Yan Y**, Rato C, Rohland L, Preissler S, Ron D. MANF antagonizes nucleotide exchange by the endoplasmic reticulum chaperone BiP. *Nat Commun* 2019; **10**: 541 [PMID: 30710085 DOI: 10.1038/s41467-019-08450-4]

24   **Harding HP**, Calfon M, Urano F, Novoa I, Ron D. Transcriptional and translational control in the Mammalian unfolded protein response. *Annu Rev Cell Dev Biol* 2002; **18**: 575-599 [PMID: 12142265 DOI: 10.1146/annurev.cellbio.18.011402.160624]

25   **Calfon M**, Zeng H, Urano F, Till JH, Hubbard SR, Harding HP, Clark SG, Ron D. IRE1 couples endoplasmic reticulum load to secretory capacity by processing the XBP-1 mRNA. *Nature* 2002; **415**: 92-96 [PMID: 11780124 DOI: 10.1038/415092a]

26   **Mizobuchi N**, Hoseki J, Kubota H, Toyokuni S, Nozaki J, Naitoh M, Koizumi A, Nagata K. ARMET is a soluble ER protein induced by the unfolded protein response via ERSE-II element. *Cell Struct Funct* 2007; **32**: 41-50 [PMID: 17507765 DOI: 10.1247/csf.07001]

27   **Tadimalla A**, Belmont PJ, Thuerauf DJ, Glassy MS, Martindale JJ, Gude N, Sussman MA, Glembotski CC. Mesencephalic astrocyte-derived neurotrophic factor is an ischemia-inducible secreted endoplasmic reticulum stress response protein in the heart. *Circ Res* 2008; **103**: 1249-1258 [PMID: 18927462 DOI: 10.1161/CIRCRESAHA.108.180679]

28   **Ayaub EA**, Tandon K, Padwal M, Imani J, Patel H, Dubey A, Mekhael O, Upagupta C, Ayoub A, Dvorkin-Gheva A, Murphy J, Kolb PS, Lhotak S, Dickhout JG, Austin RC, Kolb MRJ, Richards CD, Ask K. IL-6 mediates ER expansion during hyperpolarization of alternatively activated macrophages. *Immunol Cell Biol* 2019; **97**: 203-217 [PMID: 30298952 DOI: 10.1111/imcb.12212]

29   **Neves J**, Zhu J, Sousa-Victor P, Konjikusic M, Riley R, Chew S, Qi Y, Jasper H, Lamba DA. Immune modulation by MANF promotes tissue repair and regenerative success in the retina. *Science* 2016; **353**: aaf3646 [PMID: 27365452 DOI: 10.1126/science.aaf3646]

30   **Windmolders S**, De Boeck A, Koninckx R, Daniëls A, De Wever O, Bracke M, Hendrikx M, Hensen K, Rummens JL. Mesenchymal stem cell secreted platelet derived growth factor exerts a pro-migratory effect on resident Cardiac Atrial appendage Stem Cells. *J Mol Cell Cardiol* 2014; **66**: 177-188 [PMID: 24326234 DOI: 10.1016/j.yjmcc.2013.11.016]

31   **Bartel DP**. MicroRNAs: genomics, biogenesis, mechanism, and function. *Cell* 2004; **116**: 281-297 [PMID:

14744438 DOI: 10.1016/S0092-8674(04)00045-5]

32 **Byrd AE**, Aragon IV, Brewer JW. MicroRNA-30c-2* limits expression of proadaptive factor XBP1 in the unfolded protein response. *J Cell Biol* 2012; **196**: 689-698 [PMID: 22431749 DOI: 10.1083/jcb.201201077]

33 **Duan Q**, Chen C, Yang L, Li N, Gong W, Li S, Wang DW. MicroRNA regulation of unfolded protein response transcription factor XBP1 in the progression of cardiac hypertrophy and heart failure in vivo. *J Transl Med* 2015; **13**: 363 [PMID: 26572862 DOI: 10.1186/s12967-015-0725-4]

34 **Longa EZ**, Weinstein PR, Carlson S, Cummins R. Reversible middle cerebral artery occlusion without craniectomy in rats. *Stroke* 1989; **20**: 84-91 [PMID: 2643202 DOI: 10.1161/01.STR.20.1.84]

35 **Chen J**, Sanberg PR, Li Y, Wang L, Lu M, Willing AE, Sanchez-Ramos J, Chopp M. Intravenous administration of human umbilical cord blood reduces behavioral deficits after stroke in rats. *Stroke* 2001; **32**: 2682-2688 [PMID: 11692034 DOI: 10.1161/hs1101.098367]

36 **Bederson JB**, Pitts LH, Tsuji M, Nishimura MC, Davis RL, Bartkowski H. Rat middle cerebral artery occlusion: evaluation of the model and development of a neurologic examination. *Stroke* 1986; **17**: 472-476 [PMID: 3715945 DOI: 10.1161/01.STR.17.3.472]

37 **Swanson RA**, Morton MT, Tsao-Wu G, Savalos RA, Davidson C, Sharp FR. A semiautomated method for measuring brain infarct volume. *J Cereb Blood Flow Metab* 1990; **10**: 290-293 [PMID: 1689322 DOI: 10.1038/jcbfm.1990.47]

38 **Saura J**, Tusell JM, Serratosa J. High-yield isolation of murine microglia by mild trypsinization. *Glia* 2003; **44**: 183-189 [PMID: 14603460 DOI: 10.1002/glia.10274]

39 **Wang J**, Sun R, Li Z, Pan Y. Combined bone marrow stromal cells and oxiracetam treatments ameliorates acute cerebral ischemia/reperfusion injury through TRPC6. *Acta Biochim Biophys Sin (Shanghai)* 2019; **51**: 767-777 [PMID: 31236585 DOI: 10.1093/abbs/gmz059]

40 **Yoshida H**, Matsui T, Yamamoto A, Okada T, Mori K. XBP1 mRNA is induced by ATF6 and spliced by IRE1 in response to ER stress to produce a highly active transcription factor. *Cell* 2001; **107**: 881-891 [PMID: 11779464 DOI: 10.1016/s0092-8674(01)00611-0]

41 **Kanazawa M**, Ninomiya I, Hatakeyama M, Takahashi T, Shimohata T. Microglia and Monocytes/Macrophages Polarization Reveal Novel Therapeutic Mechanism against Stroke. *Int J Mol Sci* 2017; **18** [PMID: 29027964 DOI: 10.3390/ijms18102135]

42 **Aurora AB**, Olson EN. Immune modulation of stem cells and regeneration. *Cell Stem Cell* 2014; **15**: 14-25 [PMID: 24996166 DOI: 10.1016/j.stem.2014.06.009]

43 **Sousa-Victor P**, Jasper H, Neves J. Trophic Factors in Inflammation and Regeneration: The Role of MANF and CDNF. *Front Physiol* 2018; **9**: 1629 [PMID: 30515104 DOI: 10.3389/fphys.2018.01629]

44 **Hou C**, Wang D, Li X, He Y, Wei C, Jiang R, Liu J, Feng L, Shen Y. MANF regulates splenic macrophage differentiation in mice. *Immunol Lett* 2019; **212**: 37-45 [PMID: 31226359 DOI: 10.1016/j.imlet.2019.06.007]

45 **Li W**, Yang F, Gao J, Tang Y, Wang J, Pan Y. Over-Expression of TRPC6 via CRISPR Based Synergistic Activation Mediator in BMSCs Ameliorates Brain Injury in a Rat Model of Cerebral Ischemia/Reperfusion. *Neuroscience* 2019; **415**: 147-160 [PMID: 31369718 DOI: 10.1016/j.neuroscience.2019.06.041]

46 **Lindholm P**, Peränen J, Andressoo JO, Kalkkinen N, Kokaia Z, Lindvall O, Timmusk T, Saarma M. MANF is widely expressed in mammalian tissues and differently regulated after ischemic and epileptic insults in rodent brain. *Mol Cell Neurosci* 2008; **39**: 356-371 [PMID: 18718866 DOI: 10.1016/j.mcn.2008.07.016]

47 **Xu W**, Gao L, Li T, Zheng J, Shao A, Zhang J. Mesencephalic Astrocyte-Derived Neurotrophic Factor (MANF) Protects Against Neuronal Apoptosis via Activation of Akt/MDM2/p53 Signaling Pathway in a Rat Model of Intracerebral Hemorrhage. *Front Mol Neurosci* 2018; **11**: 176 [PMID: 29896089 DOI: 10.3389/fnmol.2018.00176]

48 **Li T**, Xu W, Gao L, Guan G, Zhang Z, He P, Xu H, Fan L, Yan F, Chen G. Mesencephalic astrocyte-derived neurotrophic factor affords neuroprotection to early brain injury induced by subarachnoid hemorrhage via activating Akt-dependent prosurvival pathway and defending blood-brain barrier integrity. *FASEB J* 2019; **33**: 1727-1741 [PMID: 30211660 DOI: 10.1096/fj.201800227RR]

49 **Chang CI**, Zoghi B, Liao JC, Kuo L. The involvement of tyrosine kinases, cyclic AMP/protein kinase A, and p38 mitogen-activated protein kinase in IL-13-mediated arginase I induction in macrophages: its implications in IL-13-inhibited nitric oxide production. *J Immunol* 2000; **165**: 2134-2141 [PMID: 10925299 DOI: 10.4049/jimmunol.165.4.2134]

50 **Shen Y**, Sun A, Wang Y, Cha D, Wang H, Wang F, Feng L, Fang S, Shen Y. Upregulation of mesencephalic astrocyte-derived neurotrophic factor in glial cells is associated with ischemia-induced glial activation. *J Neuroinflammation* 2012; **9**: 254 [PMID: 23173607 DOI: 10.1186/1742-2094-9-254]

51 **Chen L**, Feng L, Wang X, Du J, Chen Y, Yang W, Zhou C, Cheng L, Shen Y, Fang S, Li J, Shen Y. Mesencephalic astrocyte-derived neurotrophic factor is involved in inflammation by negatively regulating the NF-κB pathway. *Sci Rep* 2015; **5**: 8133 [PMID: 25640174 DOI: 10.1038/srep08133]

52 **Wang D**, Hou C, Cao Y, Cheng Q, Zhang L, Li H, Feng L, Shen Y. XBP1 activation enhances MANF expression via binding to endoplasmic reticulum stress response elements within MANF promoter region in hepatitis B. *Int J Biochem Cell Biol* 2018; **99**: 140-146 [PMID: 29649564 DOI: 10.1016/j.biocel.2018.04.007]

53 **Bartoszewski R**, Brewer JW, Rab A, Crossman DK, Bartoszewska S, Kapoor N, Fuller C, Collawn JF, Bebok Z. The unfolded protein response (UPR)-activated transcription factor X-box-binding protein 1 (XBP1) induces microRNA-346 expression that targets the human antigen peptide transporter 1 (TAP1) mRNA and governs immune regulatory genes. *J Biol Chem* 2011; **286**: 41862-41870 [PMID: 22002058 DOI: 10.1074/jbc.M111.304956]

54 **Behrman S**, Acosta-Alvear D, Walter P. A CHOP-regulated microRNA controls rhodopsin expression. *J Cell Biol* 2011; **192**: 919-927 [PMID: 21402790 DOI: 10.1083/jcb.201010055]

55 **Fang X**, Sun D, Wang Z, Yu Z, Liu W, Pu Y, Wang D, Huang A, Liu M, Xiang Z, He C, Cao L. MiR-30a Positively Regulates the Inflammatory Response of Microglia in Experimental Autoimmune Encephalomyelitis. *Neurosci Bull* 2017; **33**: 603-615 [PMID: 28717866 DOI: 10.1007/s12264-017-0153-y]

56 **Hellman M**, Arumäe U, Yu LY, Lindholm P, Peränen J, Saarma M, Permi P. Mesencephalic astrocyte-derived neurotrophic factor (MANF) has a unique mechanism to rescue apoptotic neurons. *J Biol Chem* 2011; **286**: 2675-2680 [PMID: 21047780 DOI: 10.1074/jbc.M110.146738]

57   **Lu J**, Luo L, Huang D, Liu X, Xia X, Wang Z, Lam BL, Yi J, Wen R, Li Y. Photoreceptor Protection by Mesencephalic Astrocyte-Derived Neurotrophic Factor (MANF). *eNeuro* 2018; **5** [PMID: 29687079 DOI: 10.1523/ENEURO.0109-18.2018]